Leveraging pleiotropy to discover and interpret GWAS results for sleep-associated traits

Sung Chun[1,2,3,4,25], Sebastian Akle[1,3,5,25], Athanasios Teodosiadis[3], Brian E. Cade[6,7,8], Heming Wang[6,7,8], Tamar Sofer[6,9], Daniel S. Evans[10], Katie L. Stone[10], Sina A. Gharib[11,12], Sutapa Mukherjee[13,14], Lyle J Palmer[15], David Hillman[16,17], Jerome I. Rotter[18], Craig L. Hanis[19], John A. Stamatoyannopoulos[3,20], Susan Redline[6,7,21], Chris Cotsapas[3,8,22,23,26,*], Shamil R. Sunyaev[1,3,24,26,*]

[1]Division of Genetics, Brigham and Women's Hospital, Boston, MA, USA;
[2]Division of Pulmonary Medicine, Boston Children's Hospital, Boston, MA, USA;
[3]Altius Institute for Biomedical Sciences, Seattle, WA, USA;
[4]Department of Pediatrics, Harvard Medical School, Boston, MA, USA;
[5]Department of Organismic and Evolutionary Biology, Harvard University, Cambridge, MA, USA;
[6]Division of Sleep and Circadian Disorders, Brigham and Women's Hospital, Boston, MA, USA;
[7]Division of Sleep Medicine, Harvard Medical School, Boston, MA, USA;
[8]Broad Institute of Harvard and MIT, Cambridge, MA, USA;
[9]Department of Medicine, Harvard Medical School, Boston, MA, USA;
[10]California Pacific Medical Center Research Institute, San Francisco, CA, USA;
[11]Division of Pulmonary, Critical Care, and Sleep Medicine, University of Washington, Seattle, WA, USA;
[12]Computational Medicine Core at Center for Lung Biology, University of Washington, Seattle, WA, USA;
[13]Respiratory and Sleep Services, Southern Adelaide Local Health Network, Adelaide, South Australia, Australia;
[14]Adelaide Institute for Sleep Health, Flinders University, Adelaide, South Australia, Australia;

[15]School of Public Health, University of Adelaide, Adelaide, South Australia, Australia;

[16]Centre for Sleep Science, University of Western Australia, Perth, Australia;

[17]Department of Pulmonary Physiology and Sleep Medicine, Sir Charles Gairdner Hospital, Perth, Australia;

[18]Institute for Translational Genomics and Population Sciences, Los Angeles Biomedical Research Institute at Harbor-UCLA Medical Center, Torrance, CA, USA;

[19]Department of Epidemiology, Human Genetics and Environmental Sciences, School of Public Health, University of Texas Health Science Center at Houston, Houston, TX, USA;

[20]Departments of Medicine and Genome Sciences, University of Washington, Seattle, WA, USA;

[21]Division of Pulmonary, Critical Care, and Sleep Medicine, Beth Israel Deaconess Medical Center, Boston, MA, USA;

[22]Department of Neurology, Yale School of Medicine, New Haven, CT, USA;

[23]Department of Genetics, Yale School of Medicine, New Haven, CT, USA;

[24]Department of Biomedical Informatics, Harvard Medical School, Boston, MA, USA;

[25]These authors contributed equally to this work

[26]These authors contributed equally to this work

*Correspondence: ssunyaev@hms.harvard.edu, cotsapas@broadinstitute.org

Abstract

Genetic association studies of many heritable traits resulting from physiological testing often have modest sample sizes due to the cost and burden of the required phenotyping. This reduces statistical power and limits discovery of multiple genetic associations. We present a strategy to leverage pleiotropy between traits to both discover new loci and to provide mechanistic hypotheses of the underlying pathophysiology. Specifically, we combine a colocalization test with a locus-level test of pleiotropy. In simulations, we show that this approach is highly selective for identifying true pleiotropy driven by the same causative variant, thereby improves the chance to replicate the associations in underpowered validation cohorts and leads to higher interpretability. Here, as an exemplar, we use Obstructive Sleep Apnea (OSA), a common disorder diagnosed using overnight multi-channel physiological testing. We leverage pleiotropy with relevant cellular and cardio-metabolic phenotypes and gene expression traits to map new risk loci in an underpowered OSA GWAS. We identify several pleiotropic loci harboring suggestive associations to OSA and genome-wide significant associations to other traits, and show that their OSA association replicates in independent cohorts of diverse ancestries. By investigating pleiotropic loci, our strategy allows proposing new hypotheses about OSA pathobiology across many physiological layers. For example, we identify and replicate the pleiotropy across the plateletcrit, OSA and an eQTL of DNA primase subunit 1 (*PRIM1*) in immune cells. We find suggestive links between OSA, a measure of lung function (FEV_1/FVC), and an eQTL of matrix metallopeptidase 15 (*MMP15*) in lung tissue. We also link a previously known genome-wide significant peak for OSA in the hexokinase 1 (*HK1)* locus to hematocrit and other red blood cell related traits. Thus, the analysis of pleiotropic associations has the potential to assemble diverse phenotypes into a chain of mechanistic hypotheses that provide insight into the pathogenesis of complex human diseases.

Author Summary

Large genetic studies with hundreds of thousands of patients have been successful at finding genetic variants that associate with disease traits in humans. However, smaller-scale studies can often have inadequate power to discover new genetic associations. Here, we use a small genetic study of Obstructive Sleep Apnea (OSA), to introduce a strategy that both helps find genetic associations and proposes biological hypotheses for the mechanisms behind those associations. To achieve this, we use large genetic studies carried out on traits that are related to OSA, and look for genetic variants that affect both OSA in our small study and the trait in question in the large study. By linking two or more traits at select loci, we were able to, among other results, find a locus that affects the expression of a gene in immune cells (DNA primase subunit 1), a marker of thrombotic and inflammatory processes (plateletcrit) and OSA. This results in a novel genetic association to OSA and a corresponding biological hypothesis behind its effect on OSA.

Introduction

Genome-wide association studies of human phenotypes ranging from gene expression to human diseases are now routine. Cumulatively, the data indicate that complex traits are highly polygenic [1,2], and genetic correlation between these traits indicates abundant pleiotropy [3–5]. Interpreting the plethora of results raises two major challenges: first, generating testable mechanistic hypotheses about the underlying pathophysiology; and second, increasing statistical power to identify associations in studies of traits with small or moderate sample sizes. Leveraging pleiotropy can help address both of these challenges. Previous work has demonstrated that including many correlated traits in association studies increases power to detect associations common to multiple traits [3,6,7]. This approach is largely untried in genetic investigations of Obstructive Sleep Apnea (OSA). Here, we demonstrate that using shared associations between correlated traits can identify effects in under-powered studies of OSA, and that leveraging molecular and physiological endophenotypes in this way also generates clear and testable biological hypotheses.

OSA is characterized by recurrent episodes of partial or complete obstruction of the pharyngeal airway resulting in multiple physiological disturbances, including sympathetic nervous system activation, increased energy cost of breathing, intermittent hypoxemia, and wide swings in intrathoracic pressure. This disorder is highly prevalent in the general population, affecting more than 10% of middle-aged adults, with increased prevalence observed with aging, obesity, and cardiometabolic disease, and is more common in men [8]. OSA leads to sleep disruption, particularly increased sleep fragmentation and decreased proportion of restorative stages of sleep, resulting in daytime sleepiness, impaired quality of life and cognitive deficits [9]. Moreover, OSA is associated with increased rates of hypertension, incident heart disease, stroke, diabetes, depression, certain cancers, and overall mortality [10–19]. Despite the large number of epidemiological studies indicating that OSA is closely associated with these

outcomes, there appear to be subgroup differences in susceptibility, e.g., middle-aged individuals and men are more likely to experience OSA-related cardiovascular disease in some studies than older individuals and women, respectively [20]. This underscores gaps in our knowledge of the pathophysiological pathways linking OSA to other diseases [21,22]. Pathophysiological pathways linking OSA to other diseases and factors that influence individual differences in susceptibility are poorly understood. While there are several effective treatments for OSA, including Continuous Positive Airway Pressure (CPAP), there appears to be substantial variation in overall clinical response and attenuation of cardiometabolic consequences, suggesting heterogeneity in both the etiology of the disease and susceptibility to its physiological disturbances.

Indices of OSA, including the Apnea-Hypopnea Index (AHI; the number of breathing pauses per hour of sleep), apnea event duration, indices of overnight hypoxemia, habitual snoring, and excessive daytime sleepiness, show substantial heritability in family studies [23]. Past studies have identified only a handful of associations with a variety of OSA-related traits. We have previously described a GWAS of OSA traits measured by overnight polysomnography in multi-ethnic cohorts totaling ~20,000 individuals [24]. In that study, we found two genome-wide significant multiethnic associations: variants in a locus on 10q22 were associated with indices of average and minimum SpO_2 and percentage of sleep with $SpO_2 < 90\%$, and variants in a locus on 2q12 were associated with minimum oxygen saturation (SpO_2). In another study, we identified a locus in 17p11 with a male-specific effect on AHI [25]. Furthermore, in an admixture mapping study in Hispanic/Latino Americans, we identified a locus on 2q37 associated with AHI and one in a locus on 18q21 associated with AHI and $SpO_2 < 90\%$ [26].

The low number of genetic associations reported to date only explains a small fraction of OSA trait heritability. This relative paucity of findings is driven primarily by modest sample sizes, a reflection of the expense and complexity of measuring physiological phenotypes by overnight

138 polysomnography or respiratory polygraphy. This also limits our ability to fine-map associations
139 down to causative variants and thus identify relevant genes. Data on hundreds of thousands of
140 individuals – sample sizes at which GWAS designs are well-powered to detect tens of loci and,
141 in combination with additional experiments, fine-map some of them – have yet to be collected
142 for OSA traits based on overnight polysomnography or respiratory polygraphy and may never
143 be available [1,2]. Biological interpretation of available genetic associations is further
144 complicated by the observation that most GWAS effects localize to enhancer regions and other
145 regulatory elements and are often distal to physiologically relevant genes [27,28].
146
147 Now that GWAS of massive sample sizes have been accumulated for various comorbid
148 conditions and endophenotypes related to OSA, we hypothesize that analysis of shared
149 associations across correlated traits can identify effects in underpowered studies of OSA and
150 generate clear and testable biological hypotheses. A number of computational methods
151 increase power for discovering genetic associations by capitalizing on pleiotropy between
152 disease phenotypes or between a disease and a molecular trait such as gene expression. One
153 common approach takes advantage of the genetic correlation among phenotypes [6,29–31].
154 This class of methods gains substantial additional power by pooling association signals across
155 traits. However, such methods suffer from power loss when the correlation of genetic effect
156 sizes is highly variable across the genome or limited to a subset of loci. For example, an
157 approach such as MTAG is not suitable for small GWAS studies when the assumption of the
158 homogeneity of genetic correlation is violated. The estimated genetic effect of an underpowered
159 trait can be inflated by the strong genetic signals of well-powered traits that are pooled together
160 even if the variant is not causative for the underpowered trait [6]. An alternative approach
161 analyzes individual loci to detect pleiotropic alleles, with no regard to genetic correlation
162 [4,7,32–41]. Only a handful of existing methods account for the possibility that the apparent

163 pleiotropy is driven by the linkage disequilibrium (LD) between two distinct causative variants
164 each of which drives only one phenotype [4,36–40].
165
166 In this study, we apply a colocalization method to detect shared associations between OSA and
167 other related traits. We elected Joint Likelihood Mapping method (JLIM) [39] and eCAVIAR [38]
168 as colocalization methods, but our general strategy does not depend on any specific method.
169 We focus on a set of well powered intermediate traits which have previously been implicated in
170 the pathobiology of OSA. Given prior GWAS studies suggesting the involvement of
171 inflammatory genes in OSA [42–44], and cohort studies reporting high levels of inflammation,
172 including elevations in neutrophils and monocytes in OSA [45,46], we included leukocyte and
173 platelet related traits in our pleiotropic comparisons. Similarly, we also included red blood cell
174 related traits given prior GWAS implicating iron metabolism [26] and erythrocyte function [24].
175 We will refer to these as clinical traits. In addition, OSA is associated with lung [47,48], obesity
176 and cardiovascular-related disorders [46,49–51], and we have included clinical traits that reflect
177 these overlaps, together with gene expression traits in tissues implicated in these diseases.
178
179 By linking different clinical and gene expression traits to OSA at specific loci, our analysis
180 suggests new hypotheses about OSA pathobiology across many physiological layers as well as
181 finding a new association.
182
183 **Results**
184 *Creating a framework to identify associations in underpowered GWAS through pleiotropy*
185 We used a colocalization method to identify pleiotropic loci, where a genetic effect drives
186 association to two traits. First, we selected genome-wide significant loci (association $p < 5 \times 10^{-}$
187 ^{8}) in our well-powered trait (here, a clinical trait), and from these we selected the subsets which
188 also show nominal association to OSA traits ($p < 0.01$ for any SNP in the locus). We then used
189 colocalization to directly evaluate if the association to the two traits was consistent with the

190 same underlying effect, indicating a pleiotropic effect. This two-step strategy allowed us to
191 distinguish between cases where there was association only in the clinical trait; where there was
192 a shared association in both traits; and if there were distinct associations in both traits stemming
193 from different underlying effects (Figures S1 and S2).
194
195 *Simulations*
196 We first used simulations to assess our strategy to identify true associations in an
197 underpowered study by detecting pleiotropic associations with a better-powered study of
198 another trait and following up with replication in an independent cohort. To assess sensitivity
199 and specificity, we simulated variable proportions of shared and distinct causal effects, whilst
200 assuming high polygenicity for each trait and only one causative variant per locus. We simulated
201 GWAS statistics for pairs of traits corresponding to our own study design: we simulated
202 situations where no variant is causative for an underpowered trait (H_0), where the same variant
203 is causative for the association to both traits (H_1), and where two distinct variants in LD drive
204 each of the associations at a locus (H_2) (Methods). To simulate summary statistics from a well-
205 powered GWAS (representing our clinical traits), we sampled values from a multivariate normal
206 (MVN) distribution using the local LD matrix as a variance-covariance parameter [52] with
207 clinical trait sample size of 150,000. To simulate a GWAS of limited power (representing our
208 OSA discovery cohorts), we used genotypes from ancestry-matched samples as a reference
209 from which we simulated quantitative traits in 10,000 samples as surrogates for the OSA
210 GWAS. Most overlapping associations are expected to be due to distinct variants [39]; we
211 simulated scenarios with just 5% and 20% of true associations being driven by the same variant
212 in both traits (H_1). For example, in the first case, we simulated 2,500 loci with 3.5%
213 corresponding to H_1, 66.5% corresponding to H_2 and 30% corresponding to no association in
214 the underpowered trait (H_0). The focus of our simulation study was the ability to replicate the
215 association signal for the primary phenotype in an independent cohort. This means successfully

discriminating between (H_1+H_2) and H_0. We leave the interpretability question (discriminating H_1 from H_2) to Discussion.

We tested two colocalization methods – JLIM and eCAVIAR (a popular Bayesian colocalization test) [38,39]. We also tested a popular pleiotropy-informed test, conditional false discovery rate (cFDR) [32,33]. cFDR is not based on the LD-informed colocalization of the association signals. All methods appear underpowered in the discovery dataset at a sample size typical of current genetic studies of OSA (n=10,000); the methods are only able to find associations if the observed effect is larger than the true effect (Figures S3 and S4A). Among the true associations identified by JLIM, eCAVIAR and cFDR, there is an enrichment of H_1 loci. In spite of this enrichment, many loci identified in the discovery cohort are driven by distinct variants (H_2): (for the simulation with 5% of the true associations being H_1, 54.7, 55.8 and 61.5% of loci identified by JLIM, eCAVIAR and cFDR, respectively, are H_2). At the same time, almost all proportions of successfully replicated associations are driven by the same variant (H_1) in our simulation regimes (Figures 1C-D and S4B-F).

Because the colocalization tests (such as JLIM and eCAVIAR) and cFDR are using different features of the data, we found that taking a consensus between them can effectively exclude the majority of H_2 from the analysis (Figure S3). In the intersection of JLIM and cFDR, only 3.5% of identified loci are H_2; in the intersection of eCAVIAR and cFDR, only 5.3% are H_2 (Figure S4A). Even though the elimination of H_2 loci increases the false discovery rate (fraction of H_0) in the discovery sample, it substantially increases the rate of successful replication. The main reason for the increase in the rate of successful replication is the prioritization of H_1 loci of larger true effect size and the corresponding reduction of multiple testing burden at the replication stage. The benefit of this approach increases with the fraction of loci driven by distinct effects

241 (H_2) (Figure S5). It also increased when the fraction of loci of no true effect (H_0) is low (as in the
242 case of very high polygenicity [53] (Figure S6)).
243
244 To test if the consensus method allows for more replicated loci simply due to the smaller
245 number of candidate loci, we tightened the p-value threshold of cFDR to select the same
246 number of candidates in discovery as the consensus method (Figure S7) or to control the rate of
247 H_0 loci (Figure S8). We also explored a range of other simulation conditions, including varying
248 the total number of examined well-powered trait-associated loci, correlation of effect sizes
249 between well-powered and underpowered traits, trans-ethnic validation cohort, and the
250 presence of multiple causative variants in locus (Figures S9-12). Consistently, the consensus
251 method resulted in more replicated loci than cFDR alone when the sample size is limited.
252
253 Next, we compared the rate of successful replication between the consensus approach and
254 Bayesian meta-analysis methods. In contrast to colocalization methods, the Bayesian meta-
255 analysis approach leverages the correlation of effect sizes between traits rather than SNP-level
256 colocalization of causative variants [29–31]. We chose to compare two such Bayesian meta-
257 analysis methods, MetABF and CPBayes, with the consensus approach using the simulated
258 dataset. Again, when the sample size was limited ($n < 20,000$), our consensus method found
259 more replicated associations than meta-analysis approaches (Figures S13-14). As the sample
260 size of the validation cohort increases, both MetABF and CPBayes identified more H_2 loci, which
261 led to more replicated loci than the consensus method. Since the meta-analysis methods are
262 designed for a pleiotropy analysis of more than two traits, in principle, they can boost the power
263 by using more than one well-powered trait. To test if the multi-trait meta-analysis can outperform
264 the pairwise meta-analysis, we simulated nine additional well-powered traits, generating GWAS
265 statistics for one underpowered trait and ten well-powered traits in each locus (Methods). For
266 the additional well-powered traits, we randomly decided whether the simulated causative variant
267 was to be the same as or distinct from that of the main well-powered trait. Using this simulated

268 dataset, we examined the power of the above Bayesian methods and non-parametric meta-
269 analysis (iGWAS) [7] in multi-trait and pairwise settings. Overall, we could not see a clear
270 advantage of multi-trait meta-analyses over pairwise tests in our simulated data (Figure S15).
271 Rather, particularly for CPBayes and iGWAS, multi-trait tests substantially underperformed
272 pairwise tests. This result demonstrates that for underpowered studies, the consensus approach
273 focused on SNP-level colocalization outperforms meta-analysis techniques in pairwise and
274 multi-trait settings when the association signals are driven by distinct rather than the same effect
275 in a large fraction of loci.
276
277 Finally, we found that looking at more trait combinations with more GWAS peaks results in
278 proportionally more discoveries (Figure 1E). Overall, our simulations demonstrate that casting a
279 wide net across many traits (increasing the number of GWAS peaks) and taking the consensus
280 between pleiotropy mapping methods is a viable strategy to increase discoveries in under-
281 powered studies. We therefore felt justified in pursuing this strategy using real data, to make
282 additional discoveries in traits related to OSA.
283
284 *Identifying pleiotropic associations between clinical traits and sleep apnea-related traits*
285 Based on clinical relevance [54] and heritability [23], we focused on four OSA-related traits
286 measured in five European-ancestry cohorts: the apnea-hypopnea index (AHI) [25], average
287 respiratory event (apneas or hypopneas) duration [26], and minimum and average oxygen
288 saturation (SpO_2) during sleep [24]. We used summary statistics from the remaining multi-ethnic
289 cohorts in our replication effort.
290
291 We assembled a collection of GWAS summary statistics for a total of 55 candidate intermediate
292 traits from across these physiological areas: erythroid, leukocyte and platelet counts and
293 function, from a study combining the UK Biobank and INTERVAL datasets (170,000 individuals

294 of European ancestry) [55]; cardiovascular, metabolic and respiratory traits from the UK Biobank
295 (380-450,000 European ancestry participants) [56,57], and cardio-metabolic traits (36,000
296 European ancestry participants) [58]. We then compared associations in each of these clinical
297 traits to our OSA traits (6,781 European ancestry participants; Table S1), to identify potential
298 associations in the latter. A complete list of clinical traits we considered is presented in Table
299 S2.
300
301 We tested for directional causal effects of the selected clinical traits on our OSA related traits
302 using Mendelian Randomization (MR) [59]. Due to the low sample sizes in OSA traits, no
303 comparison reached statistical significance after multiple test correction (Table S3). After
304 excluding the extended MHC region and the sex chromosomes, we identified 3,191 genome-
305 wide significant associations ($p < 5 \times 10^{-8}$) in the 55 clinical traits, of which 2,939 had a
306 corresponding suggestive association to one of the four OSA traits ($p < 0.01$ at any SNP in the
307 locus; Table S4). We then explicitly tested for evidence of pleiotropy between clinical and OSA
308 traits using JLIM (2,142 to 2,236 tests for each OSA trait). We found evidence that in 61/2,939
309 of these regions the OSA and clinical trait associations are consistent with a shared, pleiotropic
310 underlying causative variant by JLIM (false discovery rate (FDR) < 0.20) and at the same time
311 show evidence of association to OSA by cFDR (Table 1, Table S5).
312
313 To independently validate our 61 putative OSA trait associations from the discovery stage, we
314 compiled summary statistics for the same traits in 15,594 individuals of Asian, African,
315 European and Hispanic ancestries/backgrounds (Table S6). These individuals do not overlap
316 with those from the cohorts used in our colocalization analysis using JLIM. We did not attempt
317 to replicate pleiotropic associations; we only replicated the OSA association statistics. JLIM
318 relies on local LD patterns being preserved between clinical and OSA trait cohorts, so we
319 cannot use multi-ethnic data in our discovery analysis of pleiotropy. We found that 2/61 variants
320 in Table S5 show significant association with the same OSA trait as the initial observation, after

321 Bonferroni correction for the number of tests performed. The variant in SNP rs17476364 (Figure
322 2) links 11 of 12 red blood cell related clinical traits analyzed with average SpO_2 during sleep. It
323 is an intronic variant in the hexokinase 1 (*HK1*) region in chromosome 10, and has been
324 previously reported, as it reached genome-wide significance in association to minimum and
325 average SpO_2 [24]. Another variant in SNP rs2277339 is a missense coding variant in DNA
326 primase subunit 1 (*PRIM1*) in chromosome 12. It links plateletcrit (ratio of platelet volume to
327 whole blood volume, a marker of thrombotic as well as a broad range of inflammatory processes
328 [60]) to AHI. In the UK Biobank, it has documented significant associations to height, waist to
329 hip-ratio, age at menopause and multiple red blood cell related traits [61]. A further 8 variants,
330 shown in Table 1, were below nominal association p values < 0.05 in the replication set, but did
331 not survive multiple test correction.

332

333 *Incorporating gene expression to construct molecular hypotheses of sleep apnea physiology*

334 Non-coding regions with evidence of gene regulatory activity carry a large proportion of
335 heritability in most traits analyzed in large GWAS [62]. We reasoned that some OSA causative
336 variants would reside in such regulatory regions, and thus act on gene regulation. We therefore
337 sought shared associations between gene expression traits and the clinical traits for which we
338 identified a pleiotropic association in the 61 loci in Table 1 and Table S5. To do so, we compiled
339 expression quantitative trait loci (eQTL) data for protein-coding genes expressed in lung, liver,
340 spleen and skeletal muscle from individuals with European ancestry from the GTEx Project [63],
341 and monocyte, T cell and neutrophil populations in individuals from BLUEPRINT [64]. We chose
342 these tissues for potential relevance to OSA pathology: the lung is involved in OSA-related
343 hypoxemia [47,48]; previous GWAS associations have implicated the neuromuscular junction in
344 overnight SpO_2 levels, and abnormalities in upper airway muscle function are fundamental
345 mechanisms for sleep apnea [24,65]; the spleen and liver are known to mediate filtration of
346 erythrocytes, iron homeostasis and production of inflammatory cytokines; and leukocytes are

347 key modulators of inflammation, an antecedent risk factor of OSA development [66]. We
348 calculated FDR based on JLIM p-values over the 5,860 comparisons against 1,009 protein-
349 coding genes of which transcription start sites are within 1 Mb from the index SNPs of clinical
350 traits.
351
352 We were able to identify shared associations between eQTL and clinical traits in 7/61 loci (FDR
353 < 0.05; Table 2). This includes several notable examples, including rs2277339, one of our two
354 replicated SNPs (Table 1). The rs2277339 SNP is a missense variant of *PRIM1* but also an
355 eQTL for *PRIM1* levels in monocytes and T cells (Figure 3A). Another example is a locus on
356 chromosome 16 where we find that an eQTL for *MMP15* (matrix metallopeptidase 15)
357 expression in lung tissue is pleiotropic with a measure of lung function (FEV_1/FVC, the ratio of
358 forced expired volume per second to forced vital capacity), which in turn is pleiotropic with an
359 association with minimum SpO_2 during sleep (Figure 3B). The lead SNP for *MMP15*
360 (rs4784886) is marginally associated with minimum SpO_2 in the validation cohort (nominal p =
361 0.051). Overall, of the eight identified genes, four genes (*MMP15*, *SESN1*, *FOXO3* and *BRD3*)
362 are known to be induced by hypoxia and oxidative stress, and three genes (*FOXO3*, *BRD3* and
363 *GSDMA*) are implicated in inflammatory responses. The colocalization of associations to gene
364 expression in specific cell types, clinical and sleep apnea traits suggest biological hypotheses of
365 the pathophysiology underlying OSA.
366
367 We also investigated pleiotropy between gene expression traits and OSA in the three loci
368 harboring known genome-wide significant OSA associations in the discovery sample (Tables 3
369 and S7). In each locus, we compared OSA trait summary statistics to eQTLs for genes within
370 1Mb from the most associated variant, where there exists a SNP with eQTL association p-value
371 $< 5x10^{-8}$ in the locus. We replicated a previously found pleiotropic effect in a locus on
372 chromosome 17 [24], where minimum oxygen saturation (SpO_2) colocalizes with expression of

373 the epsilon subunit of the nicotinic receptor (*CHRNE*), in various tissues, including neutrophils,
374 monocytes, spleen and muscle (Figure 4).
375
376 **Discussion**

377 In our comparison of clinical (respiratory, cardiometabolic, hematologic, inflammatory) traits to
378 OSA-related traits, the strongest finding lies in an intronic region of hexokinase 1 (*HK1*) and is
379 associated with average overnight oxygen saturation level (SpO_2). This locus is pleiotropic with
380 most of the red blood cell related traits tested (Figure 2) and corresponds to one of the most
381 significant genome-wide associations we had previously reported from this data [24]. Prior to
382 this analysis, two alternative hypotheses for the etiology of this signal had been proposed: that
383 *HK1* acted by modulating inflammation, or that it affected OSA by altering erythrocyte function.
384 Our results provide evidence that is consistent with the erythrocyte pathway hypothesis.
385 Mutations in *HK1* have been implicated in anemia, together with severe hemolysis and marked
386 decreases in red blood cells [67]. As discussed previously [24], it is possible that *HK1* affects
387 the Rapoport-Luebering shunt through glycolytic pathway intermediates, which in turn mediates
388 oxygen carrying in mature erythrocytes. Factors that influence arterial oxygen levels can lead to
389 a more severe OSA phenotype (i.e., lower average levels of oxygen saturation predispose to
390 greater hypoxemia with each breathing obstruction). Lowered oxygen carrying capacity and thus
391 more tissue hypoxia could also contribute to breathing instability (and thus apneas) via Hypoxia-
392 Inducible Factor-1 (HIF-1) and enhanced carotid body sensitivity and chemoreflex activation, or
393 through long-term respiratory facilitation and plasticity [68,69].
394
395 The analysis of pleiotropy can be used to concatenate more than one phenotype to create
396 candidate "causal chains," which by linking eQTLs to well-powered traits to sleep apnea related
397 traits can hint at promising biological targets. Among the most significant results for this
398 multicomponent model is DNA primase subunit 1 (*PRIM1*). We found that a missense variant in
399 *PRIM1* colocalizes with its own expression levels in monocytes and T cells, plateletcrit, and AHI.

400 The association of this variant with AHI was replicated in an independent validation cohort. The
401 *PRIM1* deficiency is known to cause lymphopenia along with severe growth retardation,
402 microcephaly, and “triangular face” [70]. The impact of *PRIM1* on craniofacial morphology may
403 contribute to OSA by causing a narrow airway, and thereby increasing the risk of airway
404 obstruction during sleep; however, an inflammatory mechanism is also possible.
405
406 Another example of causal chains is matrix metallopeptidase 15 (*MMP15*), a gene whose
407 expression in lung tissue is affected by an eQTL that colocalizes with a lung function phenotype
408 (FEV_1/FVC) which itself colocalizes with minimum SpO_2 during sleep. Matrix metallopeptidases
409 (MMPs), a family of proteolytic enzymes that can be activated by inflammation and oxidative
410 stress, participate in and potentiate tissue remodeling by breaking down the extracellular matrix.
411 MMPs have been suggested to play an etiological role in OSA-related pathophysiological
412 responses that may lead to multiple organ dysfunction [71], and specifically, may lead to OSA
413 by contributing to abnormalities in the extracellular matrix of the skeletal muscle in the upper
414 airway, predisposing to passive airway collapse [72]. In particular, *MMP15* (membrane-type 2
415 MMP) is known to be upregulated by HIF-1α under hypoxic conditions [73,74] and is expressed
416 in alveolar epithelial cells in Idiopathic Pulmonary Fibrosis (IPF) [75], an Interstitial Lung
417 Disease (ILD) characterized by chronic inflammation, progressive formation of scar tissue and
418 decreased lung function. OSA is highly prevalent in ILD as well as associated with subclinical
419 markers of ILD [47]. OSA is also common in Chronic Obstructive Pulmonary Disease (COPD),
420 and this overlap is especially associated with more severe hypoxemia [76]. Our results suggest
421 a common causal pathway linking these lung diseases with OSA.
422
423 We also found that *GSDMA* (Gasdermin A) eQTL in T cells colocalizes with associations to the
424 lymphocyte count, AHI as well as oxygen saturation. While Gasdermin A is considered to be
425 expressed mostly in epithelial cells rather than in T cells, broadly, gasdermins mediate
426 inflammatory responses via pyroptosis, a form of programmed cell death leading to the release

427 of proinflammatory molecules, and play a key role in NLRP-inflammasome responses.
428 Increased level of gasdermin D has been shown to mediate hypoxia-related muscle injury in an
429 animal model of OSA [77]. Inflammatory mechanisms may increase risk for OSA through effects
430 on soft tissue structures in the upper airway, muscle function, and/or neural control of breathing,
431 as suggested by a prospective study of inflammation leading to higher risk of OSA [66].
432
433 Another interesting result is an eQTL in the epsilon subunit of the nicotinic acetylcholine
434 receptor *CHRNE* that colocalizes with a genome-wide significant association in minimum
435 oxygen saturation. This receptor is present at neuromuscular junctions and mutations in this
436 subunit are known to cause congenital myasthenic syndrome in humans that can result in
437 progressive respiratory impairment [78]. As discussed above, abnormal skeletal muscle
438 responses in the upper airway are considered to be central in the pathogenesis of OSA.
439
440 We have shown that we can leverage pleiotropy between OSA and physiological traits to
441 identify the known OSA association in the *HK1* locus. We could not identify two other known
442 OSA associations at 2q12 and 17p11 using this approach, as there is no apparent pleiotropy
443 between OSA and our library of clinical traits. Adding gene expression traits to this analysis
444 increases our discovery ability, as we can identify the 17p11 association as pleiotropic with an
445 eQTL for *CHRNE* in neutrophils, monocytes, spleen and muscle (Table 3). Furthermore, in
446 simulations, we showed that using a large array of clinical trait-associated loci has a potential to
447 boost the power to identify associations in underpowered studies by casting a wider net (Figure
448 1E). These results warrant further investigation on using gene expressions in diverse cell types
449 and conditions as a library of well-powered traits for underpowered association studies.
450
451 Replication in an independent cohort is frequently necessary to validate GWAS findings in small
452 discovery samples. In this study, we significantly replicate the association of two loci to OSA
453 after Bonferroni correction and identify additional eight loci that replicate only nominally but are

454 probably enriched with true positive associations to OSA (Figure S16). We randomly selected
455 28,558 unlinked autosomal SNPs ($r^2 < 0.1$ within 100kb windows) from our initial OSA GWAS in
456 individuals of European ancestry. We focused on AHI since we detected the most SNPs
457 reaching nominal replication in this trait. We found that 11,910 of these would have been
458 selected for our colocalization analysis, in line with expectation for the presence of a SNP within
459 the 100kb distance satisfying our in-sample threshold of association $p < 0.01$. Out of these,
460 6,123 had a significant out-of-sample nominal replication (association $p < 0.05$). In comparison,
461 our pleiotropy analysis results for AHI are 4.6-fold enriched at this threshold (4/20 independent
462 hits with $r^2 < 0.1$), suggesting the presence of true associations to sleep traits (one-sided Fisher
463 Exact Test $p = 0.018$). In fact, the 76/975 associations that did not show significant evidence of
464 pleiotropy were also slightly enriched for nominal replication relative to the set of randomly
465 selected variants (one-sided Fisher Exact Test $p = 0.00048$, 1.6-fold enrichment). This suggests
466 that additional pleiotropic effects – and therefore true OSA associations – remain to be
467 discovered above the FDR cutoff we applied to our colocalization results although we cannot
468 rule out the possibility that the random SNPs may not fully recapitulate the functional properties
469 of GWAS SNPs from clinical traits.
470
471 From a methodological perspective, the analysis of pleiotropy has become an important tool in
472 the analysis of complex trait genetics. Most complex traits are highly polygenic, implying that
473 many variants associated with a single trait will also be associated with other traits or will be in
474 LD with such variants. Different computational methods are required for different applications
475 and for different genetic architectures. If the goal is to increase power to detect an association
476 and the genetic correlation is broadly dispersed over many loci, methods explicitly capitalizing
477 on the broad genetic correlation are capable of producing large power gains [6,29]. In cases
478 where the majority of overlaps in GWAS association peaks between traits are driven by LD
479 between distinct causative variants, power can still be increased with the help of other methods

480 that leverage pleiotropy to reduce multiple testing burden [32,33]. Development of another
481 group of approaches was motivated by the need to link genetic associations to genes via eQTL
482 data [36,38,39] but, as shown here, these methods can be easily adapted to the analysis of
483 other traits. Because of the abundance of association signals, especially for cellular and
484 molecular traits, distinguishing between true pleiotropy due to the same underlying causative
485 variants and different causative variants in LD is important for all the applications. Therefore, in
486 our study of OSA, we selected a method that explicitly models LD structure in the locus. The
487 drawback of this choice is the need to restrict the discovery sample to a demographically
488 homogeneous subset while using the available multi-ethnic cohort for replication. While
489 colocalization tests can distinguish the same and distinct causative variants in overall, the
490 specificity is diminished in cases where association signals of two traits are driven by distinct
491 causative variants in high LD (Figure S2). For example, when the distinct causative variants are
492 in LD between 0.8 and 0.95 (3.7% of simulated data assuming the random LD distribution),
493 eCAVIAR and JLIM misclassify 1.8 and 2.3% of H_2 loci, respectively, as driven by the same
494 variant (JLIM $p < 0.01$ or at equivalent posterior probability threshold for eCAVIAR). JLIM
495 estimates accurately calibrated *p*-values under H_0 and conservative approximate *p*-values under
496 H_2. For underpowered GWAS studies, with limited sample sizes, we lowered JLIM's genetic
497 resolution parameter θ to 0.5 in this study. JLIM does not attempt to distinguish distinct
498 causative variants beyond its specified genetic resolution from the same causal effect. When
499 distinct causative variants for two traits are separated with LD $r^2 < 0.5$, JLIM maintains the ability
500 to distinguish the same and distinct effects in simulations (Figure S2 D-F). And the overall
501 specificity of JLIM to distinguish H_1 from H_2 is similar or higher compared to other colocalization
502 method such as eCAVIAR in our simulated datasets (Figure S2B).
503
504 Pleiotropy does not necessarily imply a causal relationship between phenotypes. Confounding
505 by unadjusted covariates in GWAS data can further complicate the interpretation of causal

506 chains due to the difficulty to distinguish between direct and indirect associations. Nonetheless,
507 as we demonstrate here, a shared genetic basis between OSA and organismal, cellular and
508 molecular traits can reveal new aspects of the underlying biology. This will likely be of benefit for
509 other clinically relevant traits that are difficult to study at the scale required for GWAS. Traits that
510 are burdensome or expensive to phenotype, rare diseases that are hard to sample and
511 diseases that affect under-represented populations could all lead to underpowered genetic
512 studies, which are unlikely to get dramatically higher sample sizes in the near future. Therefore,
513 there is an unmet need to optimize the signals that can be extracted from small GWAS and the
514 strategy presented here should help in achieving this goal.
515

516 **Materials and Methods**

517 *OSA Cohorts*

518 To study pleiotropic associations underlying the risk of OSA, we prepared two sets of cohorts:
519 the discovery cohorts to identify pleiotropic variants and independent replication cohorts to
520 validate their associations to OSA traits. For the discovery cohorts, we used individual-level
521 genotype data in order to determine the significance of pleiotropy by permutation (JLIM) [39]. At
522 the replication stage, we do not carry out any pleiotropy analysis, we only check for genetic
523 association to OSA, so summary-level association statistics were sufficient. In addition, we
524 restricted the genetic ancestry of GWAS discovery cohorts to that of European ancestry, to
525 match GWAS of clinical traits. This was in order to avoid potential issues due to the mismatch of
526 LD patterns in our pleiotropy analysis. In contrast, we did not require the replication cohorts to
527 have any specific ancestry. Thus, our replication cohorts included all available ethnicities.
528

529 The discovery cohorts included the subset of samples of European ancestry from the following
530 five cohorts: the Atherosclerosis Risk in Communities Study (ARIC) [79], Osteoporotic Fractures
531 in Men (MrOS) Study [80], Multi-Ethnic Study of Atherosclerosis (MESA) [81], Cardiovascular

532 Health Study (CHS) [82], and the Western Australian Sleep Health Study (WASHS) [83]. ARIC
533 is a study that investigates atherosclerosis and cardiovascular risk factors. It is one of the
534 cohorts included in the Sleep Heart Health Study, which collected polysomnography and
535 genotype data [84]. Genotype data were obtained through dbGaP (phg000035.v1.p1). MESA is
536 a population-based study focused on cardiovascular risk factors, which included participants of
537 four ethnicities: African-, Asian-, European- and Hispanic/Latino-Americans ranging from ages
538 of 45 to 86 years old. We only included samples from European-Americans in the discovery
539 cohort. Polysomnography data measuring sleep-related traits was later obtained from
540 individuals who did not use overnight oxygen, CPAP or an oral device for sleep apnea [85].
541 MrOS is a multi-center prospective epidemiological cohort assembled to examine osteoporosis,
542 fractures and prostate cancer in older males [86]. An ancillary study (MrOS Sleep) measured
543 sleep disturbances and related outcomes [87]. CHS is a cohort aimed to study coronary heart
544 disease and stroke in individuals aged 65 and older, and genotype data were obtained through
545 dbGaP (Illumina CNV370 and IBC; phg000135.v1.p1 and phg000077.v1.p1). WASHS is a
546 clinic-based study designed to examine OSA and its associated genetic risk factors in patients
547 referred to a sleep clinic in Western Australia. Not all individuals had measurements for the four
548 OSA-related traits of interest. Details on genotyping, imputation and QC procedures have been
549 previously reported [24]. See Table S1 for details.
550
551 The replication cohorts were: the Hispanic Community Health Study/Study of Latinos
552 (HCHS/SOL) [88,89], Starr County Health Studies (Starr) [90], Cleveland Family Study (CFS)
553 [91] and Framingham Heart Study (FHS) [92], in addition to non-European samples of CHS and
554 MESA. HCHS/SOL is a population-based study to examine protective and risk factors for many
555 health conditions among Hispanic/Latinos living in four urban areas within the USA (Chicago IL,
556 Miami FL, San Diego CA and Bronx NY). Starr is a cohort collected to study risk factors for
557 diabetes in a population of Mexican-Americans in Texas, later phenotyped for sleep traits [93].

558 CFS is a family-based study, which recruited patients with OSA, their relatives, and
559 neighborhood control families to study the familial and genetic basis of sleep apnea (356
560 families of African American or European American ancestry). We included only unrelated
561 individuals from CFS. FHS is an epidemiological cohort established to study cardiovascular
562 disease risk factors, using follow-up medical examinations every two years for the population of
563 European Ancestry in Framingham, MA. Data from the first Sleep Heart Health Study was
564 obtained between 1994-1998. Genotype data were obtained through dbGaP (Affymetrix 500k;
565 phg000006.v7). See Table S6 for the details of each cohort.
566
567 We examined the following four OSA-related traits in the discovery and replication cohorts:
568 minimum and average oxygen saturation (SpO_2), apnea-hypopnea index (AHI) and event
569 duration. Briefly, the minimum and average SpO_2 were calculated from oximetry-based SpO_2
570 measurements over the entire recorded sleep interval excluding occasional waking periods. AHI
571 was scored by counting the number of episodes of complete (apnea) or partial (hypopneas)
572 airflow reduction associated with $\geq$ 3% desaturation per hour of sleep. The event duration was
573 measured for the average length of apneas and hypopneas, from the nadir of the first reduced
574 breath to the nadir following the last reduced breath (in seconds). The full description of
575 phenotyping protocols are present in the original studies which first reported their genetic
576 analysis in the context of OSA [24–26]. We rank-normalized all OSA traits, separately in each
577 cohort, in order to obtain normally distributed phenotypes.
578
579 *Clinical Trait Data*
580 For clinical traits, we used GWAS summary statistics calculated for various traits in the UK
581 Biobank [56,94], blood cell-related phenotypes in a general UK population [55], and cardio-
582 metabolic phenotypes in individuals of European ancestry [58]. There is no sample overlap
583 between clinical trait GWAS data and our discovery or replication cohorts. The full list of clinical

traits is shown in Table S2. The GWAS summary statistics for UK Biobank traits and blood cell counts were downloaded from their websites. The summary statistics of cardio-metabolic traits from [58] were obtained directly from the authors.

This research was approved by Partners Healthcare IRB (protocol #2010P001765).

Identifying pleiotropic variants affecting both clinical traits and OSA

We applied Joint Likelihood Mapping (JLIM version 2.0) [39] to test whether the association signals of clinical and OSA traits were driven by a shared genetic effect. We ran JLIM only on the loci in which there was strong evidence of association to a clinical trait (genome-wide significant) and a suggestive association to the OSA trait ($p < 0.01$ at any SNP in the locus). In these loci, JLIM compares the likelihood of observed association signals under the following three competing possibilities: the OSA trait has no causative variant in the locus ("H_0"), the same OSA causative variant is shared with the clinical trait ("H_1"), and the OSA causative variant is distinct from the clinical trait causative variant ("H_2"), as shown in Figure S1. Since underlying association data have the limited genetic resolution, we test for modified hypotheses H_1^θ and H_2^θ instead of H_1 and H_2. H_1^θ represents that the causative variants of two traits are identical or in high LD ($r^2 > \theta$), and H_2^θ assumes that the causative variants are separated by the LD threshold ($r^2 < \theta$). In our simulation of underpowered GWAS (see below for the details), only a small fraction (9.0%) of loci had lead SNPs in tight LD ($r^2 > 0.8$) with causative SNPs; only 15.7% of loci had the modest LD of $r^2 > 0.5$ between lead and causative SNPs. This contrasts with well-powered GWAS data, for which, in 91.4% of simulated loci, lead SNPs were in LD of $r^2 > 0.8$ with causative SNPs. To account for this limited statistical resolution of underpowered GWAS data, we lowered θ to 0.5 from the default of 0.8 in this study.

609 JLIM calculates the ratio between the likelihood of the data under H_1^θ compared to that under H_2^θ
610 and evaluates the significance of this statistic by permuting the phenotypes simulating the lack
611 of causal effect under H_0. The false positives due to H_2^θ are indirectly controlled by the
612 asymptotically conservative behavior of JLIM: with sufficiently large effect sizes or sample sizes,
613 the cumulative distribution function of JLIM statistic shifts lower under H_2^θ than under H_0 as
614 previously shown analytically [39]. Thus, under the asymptotic condition, JLIM guarantees that
615 the p-value estimated under H_0 can be used to control for H_1^θ as well. However, under non-
616 asymptotic conditions, in particular in case of underpowered cohorts of limited sample sizes, the
617 power to distinguish H_1^θ from H_2^θ will be diminished. This reduced specificity is more pronounced
618 when the LD between distinct causative variants for two traits is substantial (See Supplements
619 of [39] for the detail). JLIM assumes that only up to one causative variant is present for each
620 trait in a locus. However, simulations showed that the accuracy of JLIM remained robust in the
621 presence of multiple causative variants in a locus (Figure S12).
622
623 To run JLIM, we used the genetic association statistics of OSA traits calculated over all common
624 SNPs in a 200kb analysis window around the focal SNP (the lead SNP of a clinical trait). We
625 derived these statistics from our discovery cohorts by combining association signals of each
626 cohort using an inverse-variance weighted meta-analysis approach. The association statistics
627 were calculated in individual cohorts by linear regression adjusting for age, sex, BMI and the top
628 three principal components. The principal components were calculated from genome-wide
629 genotype data in each cohort separately. We used mean imputation for missing covariate
630 values. Multi-allelic SNPs and rare variants with minor allele frequencies (MAF) below 0.05 were
631 excluded from the analysis. We only used variants present in all of the discovery cohorts. To
632 reflect the limited resolution for fine-mapping of causative variants in underpowered studies, we

relaxed JLIM's genetic resolution parameter θ to 0.5 from the default value of 0.8. All other parameters were set to the default. We ran JLIM only in the discovery cohorts.

JLIM 2.0 requires individual-level genetic data for underpowered traits in order to run permutations. This limits the applicability of our approach to more general cases where only summary-level data are available. The direct permutation on individual-level genetic data, however, enables robust estimation of p-values even under the vagaries of imputation noise across cohorts for underpowered traits. For the permutation procedure, we used the same pipeline described above to generate permuted association statistics for JLIM. OSA phenotypes were randomly shuffled in each cohort separately. For each permutation, the association statistics were calculated in the same way including all the covariates. Then, the cohort-level association statistics calculated on permuted data were combined across cohorts by meta-analysis. This permutation procedure was repeated up to 100,000 times, adaptively, to estimate JLIM p-values.

We accounted for the multiple testing burden with the False Discovery Rate (FDR), separately for each clinical and OSA trait combination. Specifically, we used the Benjamini-Hochberg procedure to calculate the FDR as follows:

$$FDR_{u,v}(p) = \frac{pN_{u,v}}{\left|\left\{l \mid JLIM_{u,v}(l) < p\right\}\right|}$$

where u and v indicate a combination of clinical and OSA traits, $JLIM_{u,v}(l)$ is the JLIM p-value of tested locus l, and $N_{u,v}$ is the number of loci tested between the trait pairs u and v. JLIM hits were obtained at the FDR threshold of 0.2. The JLIM/cFDR consensus was defined by the intersection between the JLIM (FDR < 0.2) and cFDR hits defined at the same p-value threshold. Specifically, given the JLIM p-value cutoff of FDR 0.2, i.e., $p_{0.2}$ such that $FDR_{u,v}(p_{0.2}) = 0.2$, the cFDR hits were defined by the association p-value below $p_{0.2}$ for an

658 OSA trait. Note that the p-value of association to a clinical trait is always ascertained to be less
659 than 5 x 10^{-8} in our analysis. The cFDR association p-values were examined at the focal SNP.
660
661 *Comparison with eCAVIAR*
662 eCAVIAR (version 2.2) was run in the default setting. The reference LD matrix was set to the LD
663 estimated from the subjects of European ancestry (n=10,000) randomly subsampled out of our
664 OSA discovery cohort. Colocalization Posterior Probability (CLPP) was calculated for lead SNPs
665 of well-powered clinical traits to identify pleiotropic loci. The CLPP thresholds were calibrated to
666 be equivalent to P-value cutoffs using unfiltered null simulation datasets (H_0), which were not
667 preconditioned on the minimum association P-values in loci.
668
669 *Replication of OSA associations in independent samples*
670 We validated the OSA associations identified in the discovery cohorts by replicating them in out-
671 of-sample multi-ethnic replication cohorts (Table S6). There was no sample overlap between
672 our discovery and replication cohorts. We combined the *p*-values of associations across the six
673 replication cohorts by applying an inverse variance-weighted meta-analysis technique. We
674 defined the *p*-value of association < 0.05 as nominal evidence of replication and the *p*-value <
675 0.05/61 as a more stringent Bonferroni-corrected replication cutoff, given that 61 independent
676 SNPs were uncovered for their pleiotropic associations to OSA in the discovery cohort (Table 1,
677 Table S5).
678
679 *Comparison of nominal replication rates with random SNPs*
680 To assess the sensitivity of our pleiotropy analysis, we compared the nominal replication rate of
681 random SNPs with that of candidate pleiotropic variants identified in the discovery cohort. We
682 started with 87,938 SNPs randomly selected across the autosomes, excluding chromosome 6 to
683 avoid the major histocompatibility complex locus. Then, we used Plink to apply LD pruning on

684 the random set of SNPs and obtained a subset of 28,558 independent SNPs. The LD pruning
685 procedure ensured that the R^2 between SNPs was less than 0.1 in the distance of 100kb in the
686 LD background of non-Finnish Europeans (n=404) from the 1000 Genomes Project. For the fair
687 comparison between random and predicted pleiotropic SNPs, we further filtered these random
688 SNPs based on the OSA association p-values in 200kb windows. Overall, we kept only 11,910
689 random independent SNPs that have an AHI-associated SNP ($P < 0.01$) within 100kb distance.
690 On all loci examined for the pleiotropy, we similarly applied the LD pruning procedure on the
691 focal SNPs to obtain a subset of independent SNPs. During the pruning steps, SNPs with more
692 significant JLIM p-values were preferentially retained. After the LD pruning, we obtained 995,
693 1,024, 967 and 961 independent SNPs for AHI, average SpO_2, minimum SpO_2, and event
694 duration, respectively; of which 20, 12, 6 and 11 SNPs are predicted to be pleiotropic in the
695 discovery cohort.
696
697 *Identifying pleiotropic variants affecting both gene expressions and OSA*
698 We used *cis*-expression quantitative trait loci (eQTLs) from the Gene-Tissue Expression project
699 (GTEx release v8) [63] and BLUEPRINT epigenome project [64], to examine pleiotropy between
700 the variation in gene expression levels and OSA phenotypes. Among the GTEx datasets, we
701 only considered liver (n=178), spleen (n=179), skeletal muscle (n=588) and lung (n=436) tissues
702 for our analysis, based on the potential relevance of these tissues to OSA and their sample
703 sizes. Again, we used eQTLs calculated only with samples of European ancestry for this
704 analysis. The genome-wide summary statistics of European American eQTLs were obtained
705 from the GTEx Consortium. For the analysis of immune cell eQTLs, we used BLUEPRINT
706 datasets which consisted of genotypes of participants and expression profiles of $CD14^+$
707 monocytes (n=191), neutrophils (n=196) and $CD4^+$ T cells (n=167). The RNA transcripts of
708 BLUEPRINT samples were derived from unstimulated primary cells collected from healthy

709 individuals of European ancestry. The genome-wide summary statistics of BLUEPRINT eQTLs
710 were downloaded from the eQTL Catalogue [95].
711
712 We start with the 61 index SNPs corresponding to the candidate pleiotropic loci identified by
713 JLIM FDR < 0.2 and cFDR consensus (Table S5). Using GTEx and BLUEPRINT eQTLs, we
714 scanned for pleiotropy between eQTLs and clinical traits. We considered all protein-coding
715 genes whose transcription start sites (TSS) were less than 1Mb away from the focal SNP of a
716 clinical trait (1,011 unique genes; 5,690 eQTLs). The protein-coding genes were defined by
717 Ensembl annotation (release 104). The genes with eQTL association *p*-value > 0.05 at all SNPs
718 in the locus were excluded due to weak evidence of association to gene expression. Overall, a
719 total of 5,860 clinical traits/eQTLs pairs (1,009 unique genes; 5,023 eQTLs) were tested for the
720 pleiotropy using JLIM in the default setting (Table 2). JLIM version 2.5 was used to test for
721 pleiotropy only using summary-level eQTL data that are publicly available. The p-values were
722 calculated by adaptive resampling (up to 10,000 iterations). The null distribution of JLIM statistic
723 was generated by random sampling of phenotypes from a normal distribution, sampling of
724 genotypes from the reference LD panel (1000 Genomes, non-Finnish Europeans), and then
725 linearly regressing the sampled phenotypes on the genotypes. Multiallelic SNPs and rare
726 variants with MAF < 0.05 were excluded from the analysis. The multiple testing burden was
727 accounted for with the False Discovery Rate (FDR) by applying the Benjamini-Hochberg
728 procedure separately to each tissue/cell type and clinical trait combination.
729
730 *Using gene expression as clinical traits*
731 In three loci with known genome-wide associations to OSA traits, we tested for pleiotropy
732 between gene expression and OSA traits using *cis*-eQTLs as clinical traits. We examined four
733 GTEx tissues and three BLUEPRINT immune cell types, similarly to the above causal chain
734 analysis. There are a total 57 eQTLs in the three loci satisfying: 1) the eQTL p-values < 5×10^{-8}
735 for a SNP within the 200kb window centered at the known OSA-associated SNP, and 2) the

736 transcription start sites being within 1 Mb from the OSA-associated SNP. Using these 57 eQTLs
737 as clinical traits, we applied JLIM in the default setting (Table S7). For the OSA traits, we used
738 the association statistics from our discovery cohorts. The JLIM FDR was calculated using the
739 Benjamini-Hochberg procedure (a total of 57 tests).
740
741 *Simulated datasets*
742 To compare the accuracy of JLIM to other methods, we simulated genetic loci with pleiotropic
743 associations under different scenarios with unbalanced sample sizes. For one of two traits, we
744 simulated a well-powered GWAS of a quantitative trait with a sample size of 150,000. For the
745 other trait, we simulated an under-powered GWAS with a much smaller sample size of 10,000.
746 To generate datasets of realistic LD backgrounds, we used real genotypes of 80 randomly
747 picked loci across the genome. Each locus was 200kb in length. Chromosome 6 and the sex
748 chromosomes were excluded from our simulations due to the difference in LD patterns from the
749 rest of genome.
750
751 In these loci, we generated 80,000 sets of association statistics under each of the following six
752 scenarios (H_0, H_1 and four configurations of H_2). For the simulations of H_0, the SNP in the
753 midpoint of the genomic segment was chosen as the causative variant for well-powered traits,
754 but no causal effect was simulated for underpowered traits. For H_1, the midpoint SNP was taken
755 as the shared causative variant for both well-powered and underpowered traits. For H_2, the
756 midpoint SNP was selected to be causal for well-powered traits, but a distinct SNP was selected
757 as the causative variant for underpowered traits. The distinct SNP was randomly chosen in the
758 intervals of LD relative to the midpoint SNP, selecting one in each of the following LD ranges: $|r|$
759 < 0.3, $0.3 < |r| < 0.6$, $0.6 < |r| < 0.8$ and $0.8 < |r| < 0.95$.
760

For each pair of causative variants, we randomly sampled the genetic effect sizes (β_1, β_2), corresponding to well-powered and underpowered traits, respectively, from the following bivariate normal distribution:

$$(\beta_1, \beta_2) \sim N(0, \Sigma)$$

$$\Sigma = \begin{bmatrix} \sigma_1^2 & \rho\sigma_1\sigma_2 \\ \rho\sigma_1\sigma_2 & \sigma_2^2 \end{bmatrix}$$

where σ_1^2 and σ_2^2 are per-SNP heritability of two traits, set to 5 x 10^{-5} under the assumptions of the heritability of 0.5, causal fraction of 0.01 and 1,000,000 independent markers across the genome. The parameter ρ was used to represent the correlation of causal effect sizes between two traits. For H_1, we generated simulated data under no correlation (ρ = 0) as well as moderate to high correlation (ρ= 0.5, 0.7 or 0.9). For H_2, we assumed ρ = 0 since the causative variants are not shared. For H_0, β_2 was set to 0.

JLIM only requires GWAS summary statistics for the well-powered trait. Therefore, for all SNPs $j = 1, \ldots, m$ in each locus, we generated summary statistics by sampling the observed association statistics $z = (z_1, \ldots, z_j, \ldots, z_m)$ from the following multivariate normal distribution [52]:

$$z \sim N\left(\sqrt{N_1} D\beta, D\right)$$

where N_1 is the GWAS sample size (150,000), m is the number of markers in the locus, D is the m x m local LD matrix, and β is the m-dimensional vector of true causal effects (on standardized genotype values) of all SNPs in the locus. Here, β was set to β_1 at the causative SNP and to 0 at all other SNPs. The *p*-values of association were calculated from the z scores as follows:

$$p_j = 2\Phi(-|z_j|)$$

where z_j is the association statistic at SNP j and Φ is the standard normal cumulative distribution function.

JLIM 2.0 requires individual-level genotype data as well as association statistics for the second trait. Therefore, for the underpowered trait, we generated a discovery cohort with simulated phenotypes for all individuals; then, we calculated the association statistics by linear regression between genotypes and phenotypes, instead of sampling the summary statistics from a multivariate normal distribution. The genotype data of 10,000 individuals were obtained by subsampling from six cohorts of European Ancestry (MESA, ARIC, MrOS, CHS, CFS, FHS and WASHS). The phenotype value y_i of each individual i was generated by random sampling from the following standard normal distribution:

$$y_i \sim N(x_i\beta_2, 1)$$

where x_i is the genotype of the causative variant in the individual i (standardized to the mean of 0 and the variance of 1). The association statistics and p-values of association were obtained by regressing the phenotypes y_i on the genotypes of each SNP in the locus. We excluded multiallelic sites and variants with MAF < 0.05 from the analysis.

The above process generated up to 480,000 sets of association data under scenarios of H_0, H_1 and H_2 in the genetic background of 80 loci (i.e., 80 x 6 x 1,000). Because of sampling noise, in a minority of simulations, association data of some loci failed to pass the genome-wide significance threshold for well-powered traits. We rejected such simulation runs to mimic our data analysis, where we only included loci in which the clinical trait association p-value was genome-wide significant. Similarly, we excluded instances where there exists no SNP with the p-value association < 0.01 for underpowered traits. In total, we retained 25,958, 31,858, 28,602,

29,131, 27,025, and 25,115 sets of association data for H_0, H_1, and H_2 of distinct causative variants in low to high LD, respectively.

Next, we estimated the distribution of LD between random pairs of SNPs in the 80 simulated loci and titrated the causative variants of H2 simulations to follow this distribution. Specifically, we subsampled H_2 datasets to fit to the following composition: 72% for |r| < 0.3, 19% for 0.3 < |r| < 0.6, 5% for 0.6 < |r| < 0.8 and 4% for 0.8 < |r| < 0.95 (Figure S2C). After this, we generated GWAS datasets of T loci by random subsampling of H_0, H_1 and H_2. T represents the total number of GWAS loci available from well-powered traits and varied from 500 to 5,000. The proportion of H_0 out of T loci varied from 0 to 30%. The relative ratios of loci simulating H_1 and H_2 were set to 1:19, 1:9, 1:4 or 1:0.

To assess the power to replicate the pleiotropic associations in independent validation cohorts, we calculated the expected association statistic z_j^v for the underpowered trait at the focal SNP j:

$$E\left[z_j^v\right] = \sqrt{N_v}\beta_2 r_{jj'}$$

where the focal SNP j was defined by the lowest p-value of association to the well-powered trait, N_v is the sample size of validation cohort for the underpowered trait, ranging from 10,000 to 35,000, β_2 is the effect size for the underpowered trait at its causative SNP j', and $r_{jj'}$ is the LD between two SNPs j and j'. For the LD backgrounds of validation cohorts, we used CEU and YRI from the 1000 Genomes Project to represent ancestry-matched and trans-ethnic validation cohorts, respectively. The expected number of replicated signals after Bonferroni correction was calculated by estimating:

$$E\left[2\Phi\left(-\left|E\left[z_j^v\right]\right|\right) < \frac{0.05}{M}\right]$$

where M is the number of pleiotropic associations found in each subsampled GWAS dataset of T loci.

Last, we also evaluated the accuracy of our method under the presence of multiple causative variants that were shared between two traits in H_1. In addition to the midpoint SNP, we randomly picked another SNP in the locus as a second shared causative variant. The effect sizes of the two causative variants for well-powered and underpowered traits were sampled from the same bivariate normal distribution. We generated GWAS datasets for the well-powered and underpowered traits in a similar manner as the simulations of single causative variants. The correlation of effect sizes between well-powered and underpowered traits (ρ) was set to 0.7 for H_1. The proportion of H_0 was assumed to be 30% of examined GWAS loci (2,500). The relative proportion of H_1 and H_2 was set to 1:19. The proportion of loci with two causative variants was set to 1/4 of all H_1 as expected under Poisson distribution with the causal fraction of 0.01.

Simulated datasets for the meta-analysis of more than two traits

GWAS data were simulated for ten well-powered and one underpowered traits under H_0, H_1 and H_2 (Figure S15A). One of the well-powered traits was ascertained to have a genome-wide significant association (the main well-powered trait). Here, we simulated association statistics only for the causative SNP of the main well-powered trait rather than simulating for entire SNPs in the locus. For simplicity of simulation, we assumed that the lead SNP of the main well-powered trait is in tight LD with its causative variant. The rest of well-powered traits have the same or distinct causative variants from the main well-powered trait. The number of additional well-powered traits simulating the same causative variants was randomly decided by sampling from a binomial distribution $Binom\left(n = 9, p = \frac{1}{20}\right)$, and the rest were assumed to have distinct causative variants. For underpowered traits, the causative variant was assumed to be absent, same or distinct from the main well-powered trait depending on whether the locus was

860 simulated under H_0, H_1 or H_2, respectively. Effect sizes of all traits sharing the same causative
861 variant were sampled together from a multivariate normal distribution with the correlation of
862 effect sizes between traits set to 0.7. Effect sizes of traits simulating distinct causative variants
863 were sampled independently and then multiplied by a random variable representing the LD
864 between causative and tested SNPs. The association statistics were generated with the sample
865 sizes of n=150,000 for well-powered traits and n=10,000 for underpowered traits. In total, 3,751,
866 613, and 6,229 sets of simulated association statistics were generated under H_0, H_1 and H_2,
867 respectively. From these simulated H_0, H_1 and H_2 datasets, GWAS datasets of 2,500 loci were
868 generated by random subsampling at the proportions of 30%, 3.5% and 66.5%, respectively
869 (H_1:H_2 ratio of 1:19). We evaluated the power to replicate the candidate pleiotropic loci using the
870 subsampled GWAS datasets (1,000 iterations). The power to replicate after Bonferroni
871 correction was estimated in the same way as other simulations. The validation cohort were
872 assumed to be of the same genetic ancestry as the discovery cohort, and the sample sizes
873 varied from n=10,000 to 35,000. For pairwise analyses, we used only the main well-powered
874 trait and underpowered trait. On the other hand, for full multi-trait analyses, we used the entire
875 data including all ten well-powered traits and one underpowered trait.

876
877 *Meta-analysis methods*

878 We benchmarked the power to replicate pleiotropic associations in underpowered cohorts by
879 applying three meta-analysis methods - MetABF, CPBayes and iGWAS - on simulated datasets.
880 We ran MetABF in the subset-exhaustive mode to scan all possible subsets of pleiotropic traits.
881 The parameter for the correlation of effect sizes was set to the known value of simulation ($\rho =$
882 0.7). MetABF was run three times with the scale parameter of causal effect sizes set to 0.1, 0.2
883 and 0.4, and the Approximate Bayes Factors (ABF) were averaged over the three runs as
884 recommended by the authors. MetABF reports the ABF relative to H_0, thus we calculated the
885 ABF of pleiotropy to the underpowered trait relative to that of no pleiotropy to the underpowered

886 trait by summing ABFs over subsets. In contrast, we ran CPBayes in the fully automatic setting.
887 All parameters of the pleiotropy were directly learned from the data. We used the PPAj
888 (Posterior Probability of Association) of the underpowered trait to identify pleiotropic
889 associations. In comparison to the two Bayesian methods, iGWAS is a non-parametric meta-
890 analysis test. We ran iGWAS in the default setting. For all three methods, candidate pleiotropic
891 associations were identified in the discovery cohort at the same p-value cutoff of 0.01. For the
892 Bayesian methods, we applied the equivalent ABF and PPAj thresholds by calibrating them to
893 have the false positive rate of 0.01 in our null simulation (H_0).
894
895

Acknowledgments

This work was supported by the National Institute of Health grant R01-HL113338. Susan Redline is partially supported by grants from the National Institutes of Health [K01-HL135405, R01-HL113338, R35-HL135818]. Shamil Sunyaev is partially supported by the National Institute of General Medical Sciences grant R35-GM127131 and the National Institute of Health grant R01-MH101244.

The Atherosclerosis Risk in Communities (ARIC) study has been funded in whole or in part with Federal funds from the National Heart, Lung, and Blood Institute, National Institutes of Health, Department of Health and Human Services (contract numbers HHSN268201700001I, HHSN268201700002I, HHSN268201700003I, HHSN268201700004I and HHSN268201700005I), R01HL087641, R01HL059367 and R01HL086694; National Human Genome Research Institute contract U01HG004402; and National Institutes of Health contract HHSN268200625226C. The authors thank the staff and participants of the ARIC study for their important contributions. Infrastructure was partly supported by Grant Number UL1RR025005, a component of the National Institutes of Health and NIH Roadmap for Medical Research.

MESA and the MESA SHARe project are conducted and supported by the National Heart, Lung, and Blood Institute (NHLBI) in collaboration with MESA investigators. Support for MESA is provided by contracts HHSN268201500003I, N01-HC-95159, N01-HC-95160, N01-HC-95161, N01-HC-95162, N01-HC-95163, N01- HC-95164, N01-HC-95165, N01-HC-95166, N01-HC-95167, N01-HC-95168, N01-HC-95169, UL1-TR-000040, UL1-TR-001079, UL1-TR-001420. MESA Family is conducted and supported by the National Heart, Lung, and Blood Institute (NHLBI) in collaboration with MESA investigators. Support is provided by grants and contracts R01HL071051, R01HL071205, R01HL071250, R01HL071251, R01HL071258, R01HL071259, and by the National Center for Research Resources, Grant UL1RR033176. The provision of genotyping data was supported in part by the National Center for Advancing Translational

923 Sciences, CTSI grant UL1TR001881, and the National Institute of Diabetes and Digestive and
924 Kidney Disease Diabetes Research Center (DRC) grant DK063491 to the Southern California
925 Diabetes Endocrinology Research Center.

926 The Osteoporotic Fractures in Men (MrOS) Study is supported by NIH funding. The following
927 institutes provide support: the National Institute on Aging (NIA), the National Institute of Arthritis
928 and Musculoskeletal and Skin Diseases (NIAMS), NCATS, and NIH Roadmap for Medical
929 Research under the following grant numbers: U01 AG027810, U01 AG042124, U01 AG042139,
930 U01 AG042140, U01 AG042143, U01 AG042145, U01 AG042168, U01 AR066160, and UL1
931 TR000128. The NHLBI provides funding for the MrOS Sleep ancillary study "Outcomes of Sleep
932 Disorders in Older Men" under the following grant numbers: R01 HL071194, R01 HL070848,
933 R01 HL070847, R01 HL070842, R01 HL070841, R01 HL070837, R01 HL070838, and R01
934 HL070839. The NIAMS provides funding for the MrOS ancillary study 'Replication of candidate
935 gene associations and bone strength phenotype in MrOS' under the grant number R01
936 AR051124. The NIAMS provides funding for the MrOS ancillary study 'GWAS in MrOS and
937 SOF' under the grant number RC2 AR058973. The investigators website can be found at
938 https://mrosonline.ucsf.edu/.

939 This CHS research was supported by NHLBI contracts HHSN268201200036C,
940 HHSN268200800007C, HHSN268201800001C, N01HC55222, N01HC85079, N01HC85080,
941 N01HC85081, N01HC85082, N01HC85083, N01HC85086; and NHLBI grants U01HL080295,
942 R01HL087652, R01HL105756, R01HL103612, R01HL120393, and U01HL130114 with
943 additional contribution from the National Institute of Neurological Disorders and Stroke (NINDS).
944 Additional support was provided through R01AG023629 from the National Institute on Aging
945 (NIA). A full list of principal CHS investigators and institutions can be found at CHS-NHLBI.org.
946 The provision of genotyping data was supported in part by the National Center for Advancing

947 Translational Sciences, CTSI grant UL1TR001881, and the National Institute of Diabetes and
948 Digestive and Kidney Disease Diabetes Research Center (DRC) grant DK063491 to the
949 Southern California Diabetes Endocrinology Research Center. The content is solely the
950 responsibility of the authors and does not necessarily represent the official views of the National
951 Institutes of Health.

952 Funding for the Western Australian Sleep Health Study was obtained from the Sir Charles
953 Gairdner and Hollywood Private Hospital Research Foundations, the Western Australian Sleep
954 Disorders Research Institute, and the Centre for Genetic Epidemiology and Biostatistics at the
955 University of Western Australia. Funding for the GWAS genotyping obtained from the Ontario
956 Institute for Cancer Research and a McLaughlin Centre Accelerator Grant from the University of
957 Toronto.

958 The Hispanic Community Health Study/Study of Latinos was carried out as a collaborative study
959 supported by contracts from the NHLBI to the University of North Carolina
960 (HHSN268201300001I / N01-HC65233), University of Miami (HHSN268201300004I / N01-
961 HC65234), Albert Einstein College of Medicine (HHSN268201300002I / N01-HC65235),
962 University of Illinois at Chicago (HHSN268201300003I), Northwestern University (N01-
963 HC65236), and San Diego State University (HHSN268201300005I / N01-HC65237). The
964 following Institutes/Centers/Offices contribute to the HCHS/SOL through a transfer of funds to
965 the NHLBI: National Institute on Minority Health and Health Disparities, National Institute on
966 Deafness and Other Communication Disorders, National Institute of Dental and Craniofacial
967 Research, National Institute of Diabetes and Digestive and Kidney Diseases, National Institute
968 of Neurological Disorders and Stroke, NIH Institution-Office of Dietary Supplements. The
969 Genetic Analysis Center at Washington University was supported by NHLBI and NIDCR
970 contracts (HHSN268201300005C AM03 and MOD03). The views expressed in this manuscript
971 are those of the authors and do not necessarily represent the views of the National Heart, Lung,

and Blood Institute; the National Institutes of Health; or the U.S. Department of Health and Human Services. The authors thank the staff and participants of HCHS/SOL for their important contributions. Investigator's website - http://www.cscc.unc.edu/hchs/

The Starr County Health Studies is supported in part by grants R01 DK073541, U01 DK085501, R01 AI085014, and R01 HL102830 from the National Institutes of Health, and funds from the University of Texas Health Science Center at Houston. We thank the field staff in Starr County for their careful collection of these data and are especially grateful to the participants who so graciously cooperated and gave of their time.

The Cleveland Family Study has been supported by National Institutes of Health grants [5-R01-HL046380-15, 5-KL2-RR024990-05, R35 HL135818, and HL113338].

The Framingham Heart Study (FHS) has been supported by contracts N01-HC-25195 and HHSN268201500001I and grant R01 HL092577. The Framingham Heart Study thanks the study participants and the multitude of investigators who over its 70 year history continue to contribute so much to further our knowledge of heart, lung, blood and sleep disorders and associated traits.

This study makes use of data generated by the BLUEPRINT Consortium. A full list of the investigators who contributed to the generation of the data is available from www.blueprint-epigenome.eu. Funding for the project was provided by the European Union's Seventh Framework Programme (FP7/2007-2013) under grant agreement no 282510 BLUEPRINT.

The Genotype-Tissue Expression (GTEx) Project was supported by the Common Fund of the Office of the Director of the National Institutes of Health, and by NCI, NHGRI, NHLBI, NIDA, NIMH, and NINDS.

995
996 **Author Contributions**

997 S.R. Sunyaev, C. Cotsapas, S. Chun, S. Akle, S. Redline conceived and designed the
998 experiment. S. Chun, S. Akle, A. Teodosiadis analyzed the data. B.E. Cade, H. Wang, T. Sofer,
999 D.S. Evans, K.L. Stone, S.A. Gharib, S. Mukherjee, L.J. Palmer, D. Hillman, J.I. Rotter, C.L.
1000 Hanis, J.A. Stamatoyannopoulos, S. Redline contributed data/analysis tools. S. Chun, S. Akle,
1001 C. Cotsapas, S.R. Sunyaev wrote the original draft. Every author reviewed and edited the
1002 manuscript.

1003

1004 **References**

1005

1006 1. Visscher PM, Wray NR, Zhang Q, Sklar P, McCarthy MI, Brown MA, et al. 10 Years of GWAS
1007 Discovery: Biology, Function, and Translation. Am J Hum Genetics. 2017;101(1):5–22.

1008 2. Zhang Y, Qi G, Park JH, Chatterjee N. Estimation of complex effect-size distributions using
1009 summary-level statistics from genome-wide association studies across 32 complex traits. Nat
1010 Genet. 2018;50(9):1318–26.

1011 3. Bulik-Sullivan B, Finucane HK, Anttila V, Gusev A, Day FR, Loh PR, et al. An atlas of genetic
1012 correlations across human diseases and traits. Nat Genet. 2015;47(11):1236–41.

1013 4. Pickrell JK, Berisa T, Liu JZ, Ségurel L, Tung JY, Hinds DA. Detection and interpretation of
1014 shared genetic influences on 42 human traits. Nat Genet. 2016;48(7):709–17.

1015 5. Shi H, Mancuso N, Spendlove S, Pasaniuc B. Local Genetic Correlation Gives Insights into the
1016 Shared Genetic Architecture of Complex Traits. Am J Hum Genetics. 2017;101(5):737–51.

1017 6. Turley P, Team 23andMe Research, Walters RK, Maghzian O, Okbay A, Lee JJ, et al. Multi-trait
1018 analysis of genome-wide association summary statistics using MTAG. Nat Genet.
1019 2018;50(2):229–37.

1020 7. Fortney K, Dobriban E, Garagnani P, Pirazzini C, Monti D, Mari D, et al. Genome-Wide Scan
1021 Informed by Age-Related Disease Identifies Loci for Exceptional Human Longevity. Plos Genet.
1022 2015;11(12):e1005728.

1023 8. Peppard PE, Hagen EW. The Last 25 Years of Obstructive Sleep Apnea Epidemiology—and the
1024 Next 25? Am J Resp Crit Care. 2017;197(3):310–2.

1025 9. Olaithe M, Bucks RS. Executive Dysfunction in OSA Before and After Treatment: A Meta-
1026 Analysis. Sleep. 2013;36(9):1297–305.

1027 10. Gami AS, Hodge DO, Herges RM, Olson EJ, Nykodym J, Kara T, et al. Obstructive sleep apnea,
1028 obesity, and the risk of incident atrial fibrillation. J Am Coll Cardiol. 2007;49(5):565–71.

1029 11. Gozal D, Ham SA, Mokhlesi B. Sleep Apnea and Cancer: Analysis of a Nationwide Population
1030 Sample. Sleep. 2016;39(8):1493–500.

1031 12. Nieto FJ, Peppard PE, Young T, Finn L, Hla KM, Farré R. Sleep-disordered breathing and
1032 cancer mortality: results from the Wisconsin Sleep Cohort Study. Am J Resp Crit Care.
1033 2012;186(2):190–4.

1034 13. Kendzerska T, Gershon AS, Hawker G, Leung RS, Tomlinson G. Obstructive Sleep Apnea and
1035 Risk of Cardiovascular Events and All-Cause Mortality: A Decade-Long Historical Cohort Study.
1036 Plos Med. 2014;11(2):e1001599.

1037 14. Oldenburg O, Wellmann B, Buchholz A, Bitter T, Fox H, Thiem U, et al. Nocturnal
1038 hypoxaemia is associated with increased mortality in stable heart failure patients. Eur Heart J.
1039 2016;37(21):1695–703.

1040 15. Nagayoshi M, Punjabi NM, Selvin E, Pankow JS, Shahar E, Iso H, et al. Obstructive sleep
1041 apnea and incident type 2 diabetes. Sleep Med. 2016;25:156–61.

1042 16. BaHammam AS, Kendzerska T, Gupta R, Ramasubramanian C, Neubauer DN, Narasimhan M,
1043 et al. Comorbid depression in obstructive sleep apnea: an under-recognized association. Sleep
1044 Breath. 2016;20(2):447–56.

1045 17. Torres G, Sánchez-de-la-Torre M, Barbé F. Relationship Between OSA and Hypertension.
1046 Chest. 2015;148(3):824–32.

1047 18. Somers VK, White DP, Amin R, Abraham WT, Costa F, Culebras A, et al. Sleep Apnea and
1048 Cardiovascular Disease An American Heart Association/American College of Cardiology
1049 Foundation Scientific Statement From the American Heart Association Council for High Blood
1050 Pressure Research Professional Education Committee, Council on Clinical Cardiology, Stroke
1051 Council, and Council on Cardiovascular Nursing In Collaboration With the National Heart, Lung,
1052 and Blood Institute National Center on Sleep Disorders Research (National Institutes of Health).
1053 J Am Coll Cardiol. 2008;52(8):686–717.

1054 19. Redline S, Yenokyan G, Gottlieb DJ, Shahar E, O'Connor GT, Resnick HE, et al. Obstructive
1055 Sleep Apnea–Hypopnea and Incident Stroke. Am J Resp Crit Care. 2010;182(2):269–77.

1056 20. Gottlieb DJ, Yenokyan G, Newman AB, O'Connor GT, Punjabi NM, Quan SF, et al. Prospective
1057 Study of Obstructive Sleep Apnea and Incident Coronary Heart Disease and Heart Failure.
1058 Circulation. 2010;122(4):352–60.

1059 21. Mukherjee S, Saxena R, Palmer LJ. The genetics of obstructive sleep apnoea. Respirology.
1060 2018;23(1):18–27.

1061 22. Palmer LJ, Redline S. Genomic approaches to understanding obstructive sleep apnea. Resp
1062 Physiol Neurobi. 2003;135(2):187–205.

1063 23. Liang J, Cade BE, Wang H, Chen H, Gleason KJ, Larkin EK, et al. Comparison of Heritability
1064 Estimation and Linkage Analysis for Multiple Traits Using Principal Component Analyses. Genet
1065 Epidemiol. 2016;40(3):222–32.

1066 24. Cade BE, Chen H, Stilp AM, Louie T, Ancoli-Israel S, Arens R, et al. Associations of variants In
1067 the hexokinase 1 and interleukin 18 receptor regions with oxyhemoglobin saturation during
1068 sleep. Plos Genet. 2019;15(4):e1007739.

1069 25. Chen H, Cade BE, Gleason KJ, Bjonnes AC, Stilp AM, Sofer T, et al. Multiethnic Meta-Analysis
1070 Identifies \textitRAI1 as a Possible Obstructive Sleep Apnea–related Quantitative Trait Locus in
1071 Men. Am J Resp Cell Mol. 2018;58(3):391–401.

1072 26. Wang H, Cade BE, Sofer T, Sands SA, Chen H, Browning SR, et al. Admixture mapping
1073 identifies novel loci for obstructive sleep apnea in Hispanic/Latino Americans. Hum Mol Genet.
1074 2019;28(4):675–87.

1075 27. Gusev A, Lee SH, Trynka G, Finucane H, Vilhjálmsson BJ, Xu H, et al. Partitioning Heritability
1076 of Regulatory and Cell-Type-Specific Variants across 11 Common Diseases. Am J Hum Genetics.
1077 2014;95(5):535–52.

1078 28. Maurano MT, Humbert R, Rynes E, Thurman RE, Haugen E, Wang H, et al. Systematic
1079 Localization of Common Disease-Associated Variation in Regulatory DNA. Science.
1080 2012;337(6099):1190–5.

1081 29. Trochet H, Pirinen M, Band G, Jostins L, McVean G, Spencer CCA. Bayesian meta-analysis
1082 across genome-wide association studies of diverse phenotypes. Genet Epidemiol.
1083 2019;43(5):532–47.

1084 30. Majumdar A, Haldar T, Bhattacharya S, Witte JS. An efficient Bayesian meta-analysis
1085 approach for studying cross-phenotype genetic associations. Plos Genet. 2018;14(2):e1007139.

1086 31. Urbut SM, Wang G, Carbonetto P, Stephens M. Flexible statistical methods for estimating
1087 and testing effects in genomic studies with multiple conditions. Nat Genet. 2019;51(1):187–95.

1088 32. Andreassen OA, Djurovic S, Thompson WK, Schork AJ, Kendler KS, O'Donovan MC, et al.
1089 Improved Detection of Common Variants Associated with Schizophrenia by Leveraging
1090 Pleiotropy with Cardiovascular-Disease Risk Factors. Am J Hum Genetics. 2013;92(2):197–209.

1091 33. Andreassen OA, Thompson WK, Schork AJ, Ripke S, Mattingsdal M, Kelsoe JR, et al.
1092 Improved Detection of Common Variants Associated with Schizophrenia and Bipolar Disorder
1093 Using Pleiotropy-Informed Conditional False Discovery Rate. Plos Genet. 2013;9(4):e1003455.

1094 34. Wang Y, Thompson WK, Schork AJ, Holland D, Chen CH, Bettella F, et al. Leveraging
1095 Genomic Annotations and Pleiotropic Enrichment for Improved Replication Rates in
1096 Schizophrenia GWAS. Plos Genet. 2016;12(1):e1005803.

1097 35. Liley J, Wallace C. A Pleiotropy-Informed Bayesian False Discovery Rate Adapted to a Shared
1098 Control Design Finds New Disease Associations From GWAS Summary Statistics. Plos Genet.
1099 2015;11(2):e1004926.

1100 36. Giambartolomei C, Vukcevic D, Schadt EE, Franke L, Hingorani AD, Wallace C, et al. Bayesian
1101 Test for Colocalisation between Pairs of Genetic Association Studies Using Summary Statistics.
1102 Plos Genet. 2014;10(5):e1004383.

1103 37. Giambartolomei C, Liu JZ, Zhang W, Hauberg M, Shi H, Boocock J, et al. A Bayesian
1104 framework for multiple trait colocalization from summary association statistics. Bioinformatics.
1105 2018;34(15):2538–45.

1106 38. Hormozdiari F, van de Bunt M, Segrè AV, Li X, Joo JWJ, Bilow M, et al. Colocalization of
1107 GWAS and eQTL Signals Detects Target Genes. Am J Hum Genetics. 2016;99(6):1245–60.

1108 39. Chun S, Casparino A, Patsopoulos NA, Croteau-Chonka DC, Raby BA, Jager PLD, et al. Limited
1109 statistical evidence for shared genetic effects of eQTLs and autoimmune-disease-associated loci
1110 in three major immune-cell types. Nat Genet. 2017;49(4):600–5.

1111 40. Zhu Z, Zhang F, Hu H, Bakshi A, Robinson MR, Powell JE, et al. Integration of summary data
1112 from GWAS and eQTL studies predicts complex trait gene targets. Nat Genet. 2016;48(5):481–7.

1113 41. Gusev A, Ko A, Shi H, Bhatia G, Chung W, Penninx BWJH, et al. Integrative approaches for
1114 large-scale transcriptome-wide association studies. Nat Genet. 2016;48(3):245–52.

1115 42. Larkin EK, Patel SR, Zhu X, Tracy RP, Jenny NS, Reiner AP, et al. A Study of The Relationship
1116 between The Interleukin-6 Gene and Obstructive Sleep Apnea. Clin Transl Sci. 2010;3(6):337–9.

1117 43. Larkin EK, Patel SR, Goodloe RJ, Li Y, Zhu X, Gray-McGuire C, et al. A candidate gene study of
1118 obstructive sleep apnea in European Americans and African Americans. Am J Resp Crit Care.
1119 2010;182(7):947–53.

1120 44. Patel SR, Goodloe R, De G, Kowgier M, Weng J, Buxbaum SG, et al. Association of genetic
1121 loci with sleep apnea in European Americans and African-Americans: the Candidate Gene
1122 Association Resource (CARe). Plos One. 2012;7(11):e48836.

1123 45. Geovanini GR, Wang R, Weng J, Tracy R, Jenny NS, Goldberger AL, et al. Elevations in
1124 neutrophils with obstructive sleep apnea: The Multi-Ethnic Study of Atherosclerosis (MESA). Int
1125 J Cardiol. 2018;257:318–23.

1126 46. Geovanini GR, Wang R, Weng J, Jenny NS, Shea S, Allison M, et al. Association between
1127 Obstructive Sleep Apnea and Cardiovascular Risk Factors: Variation by Age, Sex, and Race. The
1128 Multi-Ethnic Study of Atherosclerosis. Ann Am Thorac Soc. 2018;15(8):970–7.

1129 47. Kim JS, Podolanczuk AJ, Borker P, Kawut SM, Raghu G, Kaufman JD, et al. Obstructive Sleep
1130 Apnea and Subclinical Interstitial Lung Disease in the Multi-Ethnic Study of Atherosclerosis
1131 (MESA). Ann Am Thorac Soc. 2017;14(12):1786–95.

1132 48. Lederer DJ, Jelic S, Basner RC, Ishizaka A, Bhattacharya J. Circulating KL-6, a Biomarker of
1133 Lung Injury, in Obstructive Sleep Apnea. Eur Respir J. 2009;33(4):793–6.

1134 49. McNicholas WT. Comorbid obstructive sleep apnoea and chronic obstructive pulmonary
1135 disease and the risk of cardiovascular disease. Journal of Thoracic Disease. 2018;1(1):S4253–61-
1136 -S4261.

1137 50. McAlpine CS, Kiss MG, Rattik S, He S, Vassalli A, Valet C, et al. Sleep modulates
1138 haematopoiesis and protects against atherosclerosis. Nature. 2019;566(7744):383–7.

1139 51. Xie J, Li F, Wu X, Hou W. Prevalence of pulmonary embolism in patients with obstructive
1140 sleep apnea and chronic obstructive pulmonary disease: The overlap syndrome. Heart Lung.
1141 2019;48(3):261–5.

1142 52. Conneely KN, Boehnke M. So Many Correlated Tests, So Little Time! Rapid Adjustment of P
1143 Values for Multiple Correlated Tests. Am J Hum Genetics. 2007;81(6):1158–68.

1144 53. Boyle EA, Li YI, Pritchard JK. An Expanded View of Complex Traits: From Polygenic to
1145 Omnigenic. Cell. 2017;169(7):1177–86.

1146 54. Butler MP, Emch JT, Rueschman M, Sands SA, Shea SA, Wellman A, et al. Apnea-Hypopnea
1147 Event Duration Predicts Mortality in Men and Women in the Sleep Heart Health Study. Am J
1148 Resp Crit Care. 2019;199(7):903–12.

1149 55. Astle WJ, Elding H, Jiang T, Allen D, Ruklisa D, Mann AL, et al. The Allelic Landscape of
1150 Human Blood Cell Trait Variation and Links to Common Complex Disease. Cell.
1151 2016;167(5):1415-1429.e19.

1152 56. Loh PR, Kichaev G, Gazal S, Schoech AP, Price AL. Mixed-model association for biobank-scale
1153 datasets. Nat Genet. 2018;50(7):906–8.

1154 57. Bycroft C, Freeman C, Petkova D, Band G, Elliott LT, Sharp K, et al. The UK Biobank resource
1155 with deep phenotyping and genomic data. Nature. 2018;562(7726):203–9.

1156 58. Iotchkova V, Huang J, Morris JA, Jain D, Barbieri C, Walter K, et al. Discovery and refinement
1157 of genetic loci associated with cardiometabolic risk using dense imputation maps. Nat Genet.
1158 2016;48(11):1303–12.

1159 59. Hemani G, Zheng J, Elsworth B, Wade KH, Haberland V, Baird D, et al. The MR-Base platform
1160 supports systematic causal inference across the human phenome. Elife. 2018;7:e34408.

1161 60. Gros A, Ollivier V, Ho-Tin-Noé B. Platelets in Inflammation: Regulation of Leukocyte
1162 Activities and Vascular Repair. Front Immunol. 2015;5:678.

1163 61. Kichaev G, Bhatia G, Loh PR, Gazal S, Burch K, Freund MK, et al. Leveraging Polygenic
1164 Functional Enrichment to Improve GWAS Power. Am J Hum Genetics. 2019;104(1):65–75.

1165 62. Finucane HK, Bulik-Sullivan B, Gusev A, Trynka G, Reshef Y, Loh PR, et al. Partitioning
1166 heritability by functional annotation using genome-wide association summary statistics. Nat
1167 Genet. 2015;47(11):1228–35.

1168 63. Consortium TGte. The GTEx Consortium atlas of genetic regulatory effects across human
1169 tissues. Science. 2020;369(6509):1318–30.

1170 64. Chen L, Ge B, Casale FP, Vasquez L, Kwan T, Garrido-Martín D, et al. Genetic Drivers of
1171 Epigenetic and Transcriptional Variation in Human Immune Cells. Cell. 2016;167(5):1398-
1172 1414.e24.

1173 65. Owens RL, Edwards BA, Eckert DJ, Jordan AS, Sands SA, Malhotra A, et al. An Integrative
1174 Model of Physiological Traits Can be Used to Predict Obstructive Sleep Apnea and Response to
1175 Non Positive Airway Pressure Therapy. Sleep. 2015;38(6):961–70.

1176 66. Huang T, Goodman M, Li X, Sands SA, Li J, Stampfer MJ, et al. C-reactive Protein and Risk of
1177 OSA in Four US Cohorts. Chest. 2021;159(6):2439–48.

1178 67. Wijk R van, Solinge WW van. The energy-less red blood cell is lost: erythrocyte enzyme
1179 abnormalities of glycolysis. Blood. 2005;106(13):4034–42.

1180 68. Powell FL, Fu Z. HIF-1 and ventilatory acclimatization to chronic hypoxia. Resp Physiol
1181 Neurobi. 2008;164(1–2):282–7.

1182 69. Devinney MJ, Nichols NL, Mitchell GS. Sustained Hypoxia Elicits Competing Spinal
1183 Mechanisms of Phrenic Motor Facilitation. J Neurosci. 2016;36(30):7877–85.

1184 70. Parry DA, Tamayo-Orrego L, Carroll P, Marsh JA, Greene P, Murina O, et al. PRIM1 deficiency
1185 causes a distinctive primordial dwarfism syndrome. Gene Dev. 2020;34(21–22):1520–33.

1186 71. Franczak A, Bil-Lula I, Sawicki G, Fenton M, Ayas N, Skomro R. Matrix metalloproteinases as
1187 possible biomarkers of obstructive sleep apnea severity – a systematic review. Sleep Med Rev.
1188 2019;46:9–16.

1189 72. Dantas DA da S, Mauad T, Silva LFF, Lorenzi-Filho G, Formigoni GGS, Cahali MB. The
1190 Extracellular Matrix of the Lateral Pharyngeal Wall in Obstructive Sleep Apnea. Sleep.
1191 2012;35(4):483–90.

1192 73. Rosa DP da, Forgiarini LF, Baronio D, Feijó CA, Martinez D, Marroni NP. Simulating Sleep
1193 Apnea by Exposure to Intermittent Hypoxia Induces Inflammation in the Lung and Liver. Mediat
1194 Inflamm. 2012;2012:879419.

1195 74. Zhu S, Zhou Y, Wang L, Zhang J, Wu H, Xiong J, et al. Transcriptional upregulation of MT2-
1196 MMP in response to hypoxia is promoted by HIF-1α in cancer cells. Mol Carcinogen.
1197 2011;50(10):770–80.

1198 75. García-Alvarez J, Ramirez R, Sampieri CL, Nuttall RK, Edwards DR, Selman M, et al.
1199 Membrane type-matrix metalloproteinases in idiopathic pulmonary fibrosis. Sarcoidosis Vasc
1200 Diffuse Lung Dis Official J Wasog World Assoc Sarcoidosis Other Granulomatous Disord.
1201 2006;23(1):13–21.

1202 76. Owens RL, Malhotra A. Sleep-disordered breathing and COPD: the overlap syndrome. Respir
1203 Care. 2010;55(10):1333–44; discussion 1344-6.

1204 77. Yu LM, Zhang WH, Han XX, Li YY, Lu Y, Pan J, et al. Hypoxia-Induced ROS Contribute to
1205 Myoblast Pyroptosis during Obstructive Sleep Apnea via the NF-κB/HIF-1α Signaling Pathway.
1206 Oxid Med Cell Longev. 2019;2019:4596368.

1207 78. Estephan E de P, Sobreira CF da R, Santos ACJD, Tomaselli PJ, Marques W, Ortega RPM, et
1208 al. A common CHRNE mutation in Brazilian patients with congenital myasthenic syndrome. J
1209 Neurol. 2018;265(3):708–13.

1210 79. The Atherosclerosis Risk in Communities (ARIC) Study: design and objectives. The ARIC
1211 investigators. Am J Epidemiol. 1989;129(4):687–702.

1212 80. Orwoll E, Blank JB, Barrett-Connor E, Cauley J, Cummings S, Ensrud K, et al. Design and
1213 baseline characteristics of the osteoporotic fractures in men (MrOS) study--a large

1214 observational study of the determinants of fracture in older men. Contemp Clin Trials.
1215 2005;26(5):569–85.

1216 81. Bild DE, Bluemke DA, Burke GL, Detrano R, Roux AVD, Folsom AR, et al. Multi-Ethnic Study
1217 of Atherosclerosis: objectives and design. Am J Epidemiol. 2002;156(9):871–81.

1218 82. Fried LP, Borhani NO, Enright P, Furberg CD, Gardin JM, Kronmal RA, et al. The
1219 Cardiovascular Health Study: design and rationale. Ann Epidemiol. 1991;1(3):263–76.

1220 83. Mukherjee S, Hillman D, Lee J, Fedson A, Simpson L, Ward K, et al. Cohort profile: the
1221 Western Australian Sleep Health Study. Sleep Breath. 2012;16(1):205–15.

1222 84. Quan SF, Howard BV, Iber C, Kiley JP, Nieto FJ, O'Connor GT, et al. The Sleep Heart Health
1223 Study: design, rationale, and methods. Sleep. 1997;20(12):1077–85.

1224 85. Chen X, Wang R, Zee P, Lutsey PL, Javaheri S, Alcántara C, et al. Racial/Ethnic Differences in
1225 Sleep Disturbances: The Multi-Ethnic Study of Atherosclerosis (MESA). Sleep. 2015;38(6):877–
1226 88.

1227 86. Blank JB, Cawthon PM, Carrion-Petersen ML, Harper L, Johnson JP, Mitson E, et al. Overview
1228 of recruitment for the osteoporotic fractures in men study (MrOS). Contemp Clin Trials.
1229 2005;26(5):557–68.

1230 87. Mehra R, Stone KL, Blackwell T, Israel SA, Dam TTL, Stefanick ML, et al. Prevalence and
1231 Correlates of Sleep-Disordered Breathing in Older Men: Osteoporotic Fractures in Men Sleep
1232 Study. J Am Geriatr Soc. 2007;55(9):1356–64.

1233 88. Sorlie PD, Avilés-Santa LM, Wassertheil-Smoller S, Kaplan RC, Daviglus ML, Giachello AL, et
1234 al. Design and implementation of the Hispanic Community Health Study/Study of Latinos. Ann
1235 Epidemiol. 2010;20(8):629–41.

1236 89. Redline S, Sotres-Alvarez D, Loredo J, Hall M, Patel SR, Ramos A, et al. Sleep-disordered
1237 Breathing in Hispanic/Latino Individuals of Diverse Backgrounds. The Hispanic Community
1238 Health Study/Study of Latinos. Am J Resp Crit Care. 2014;189(3):335–44.

1239 90. Hanis CL, Ferrell RE, Barton SA, Aguilar L, Garza-Ibarra A, Tulloch BR, et al. Diabetes among
1240 Mexican Americans in Starr County, Texas. Am J Epidemiol. 1983;118(5):659–72.

1241 91. Redline S, Tishler PV, Tosteson TD, Williamson J, Kump K, Browner I, et al. The familial
1242 aggregation of obstructive sleep apnea. Am J Resp Crit Care. 1995;151(3 Pt 1):682–7.

1243 92. Feinleib M. The Framingham Study: sample selection, follow-up, and methods of analyses.
1244 National Cancer Inst Monogr. 1985;67:59–64.

93. Hanis CL, Redline S, Cade BE, Bell GI, Cox NJ, Below JE, et al. Beyond type 2 diabetes, obesity and hypertension: an axis including sleep apnea, left ventricular hypertrophy, endothelial dysfunction, and aortic stiffness among Mexican Americans in Starr County, Texas. Cardiovasc Diabetol. 2016;15(1):86.

94. Sudlow C, Gallacher J, Allen N, Beral V, Burton P, Danesh J, et al. UK Biobank: An Open Access Resource for Identifying the Causes of a Wide Range of Complex Diseases of Middle and Old Age. Plos Med. 2015;12(3):e1001779.

95. Kerimov N, Hayhurst JD, Peikova K, Manning JR, Walter P, Kolberg L, et al. A compendium of uniformly processed human gene expression and splicing quantitative trait loci. Nat Genet. 2021;53(9):1290–9.

Supporting Information

Figure S1. Schematic of JLIM analysis.

Figure S2. Sensitivity for H_1 and specificity to distinguish H_1 from H_2.

Figure S3. Winner's curse.

Figure S4. The number of loci that were identified in simulated discovery and validation cohorts, broken down by the configuration of causative variants.

Figure S5. The projected number of replicated loci in simulations, varying the relative ratio between H_1 and H_2.

Figure S6. The projected number of replicated loci in simulations, varying the proportion of H_0 loci.

Figure S7. The projected number of replicated loci in simulations where the cFDR threshold was tightened to identify the same number of candidate loci as the JLIM/cFDR consensus method in a discovery cohort.

Figure S8. The projected number of replicated loci in simulations where the cFDR threshold was calibrated to have the same false positive rate for H_0.

Figure S9. The projected number of replicated loci in simulations where the number of association peaks available from well-powered traits varied.

Figure S10. The projected number of replicated loci in simulations where the correlation of effect sizes for H_1 varied.

Figure S11. The projected number of replicated loci in simulations of trans-ethnic replication.

Figure S12. The projected number of replicated loci in simulations of multiple causative variants for H1.

Figure S13. Comparison with Bayesian meta-analysis methods with a validation cohort from the same ancestry.

Figure S14. Comparison with Bayesian meta-analysis methods with a validation cohort from the different ancestry (YRI).

Figure S15. Simulated power of multi-trait meta-analysis compared to pairwise analysis.

Figure S16. Pleiotropic loci identified by the intersection of JLIM and cFDR are enriched with SNPs that nominally replicate out of sample.

Table S1. Sample sizes of discovery cohorts used for the pleiotropy analysis.

Table S2. Clinical traits used for the pleiotropy analysis.

Table S3. Mendelian randomization analysis p-values testing effect of exposure on outcome.

Table S4. Overall number of total tests, identified pleiotropic loci, and nominally replicated signals.

Table S5. List of identified pleiotropic loci and their replication p-values for the corresponding OSA traits (JLIM FDR < 0.2).

Table S6. Sample sizes of validation cohorts used for the replication study.

Table S7. Full results of pleiotropy tests between eQTLs and OSA traits in three known OSA GWAS loci at the eQTL p-value < 5e-8.

Figures and Tables

Figure 1

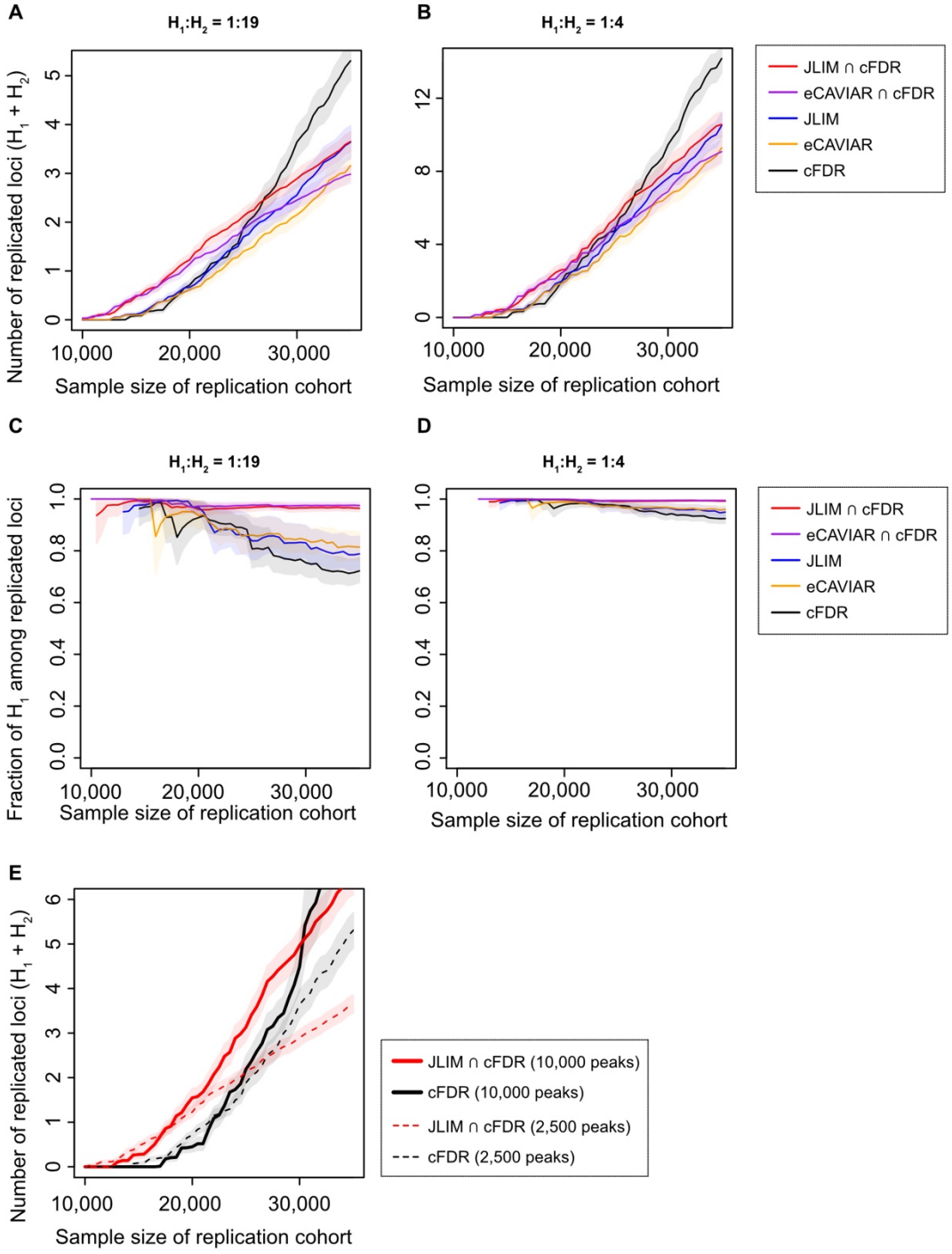

Figure 1. The projected number of replicated loci and proportion of shared causative variants among the replicated loci.

A total of 2,500 association peaks from well-powered GWAS studies (n=150,000) were tested for the shared effect in simulated discovery cohorts (n=10,000), and then select loci were tested for replication in simulated validation cohorts of the same genetic ancestry (n=10,000-35,000).

The candidate loci were identified by conditional false discovery rate (cFDR), colocalization tests (JLIM and eCAVIAR), or the intersection of cFDR and colocalization test. The P-value cutoff was set to 0.01 for cFDR and JLIM, and for eCAVIAR, the equivalent posterior threshold was calibrated using H_0 simulation data. The 2,500 GWAS peaks consist of the loci simulating no causal effect for underpowered traits (H_0) and those simulating the same causal effect between two traits (H_1) or distinct causal effects (H_2). The H_1:H_2 ratio was set to 1:19 (**A** and **C**) or 1:4 (**B** and **D**). The effect sizes of causative variants are correlated ($\rho = 0.7$) under H_1 but uncorrelated under H_2. Bonferroni correction was applied on replication tests. In Panel **E**, we contrast the number of replicated loci expected in Panel **A** (dashed line) with a more extreme scenario (10,000 GWAS peaks, consisting of 2,500 with H_1:H_2 of 1:19 and 7,500 with H_1:H_2 of 1:39; solid lines). In all, the proportion of H_0 was set to 30% of all examined loci. The shaded area denotes the 95% CIs.

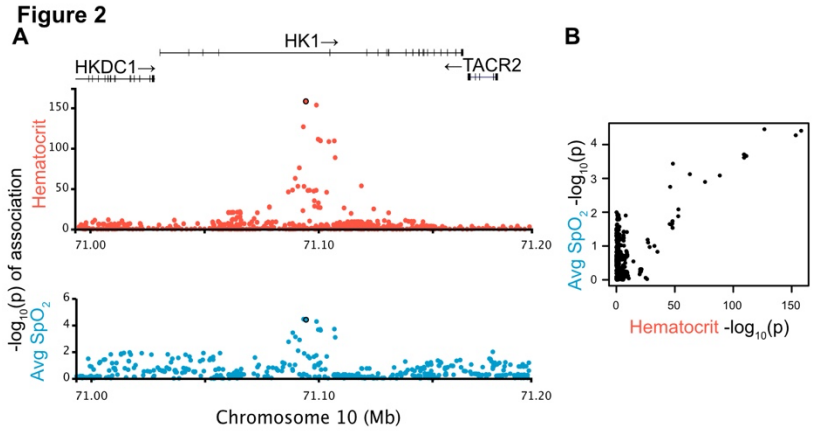

Figure 2. Pleiotropy at HK1 locus.

A) Putatively pleiotropic locus linking a clinical trait (hematocrit) with an OSA trait (average SpO_2). The evidence of shared effect between the clinical and OSA traits is significant (JLIM p = 4.2×10^{-4}, FDR = 0.017). This SpO_2 association replicates in validation cohorts after Bonferroni correction of 61 tests (p = 8.5×10^{-5}). **B)** Pairwise comparison of $-\log_{10}$(p-values) between two traits confirms that the association signals are driven by the shared underlying effect. Each dot represents a SNP in the tested locus.

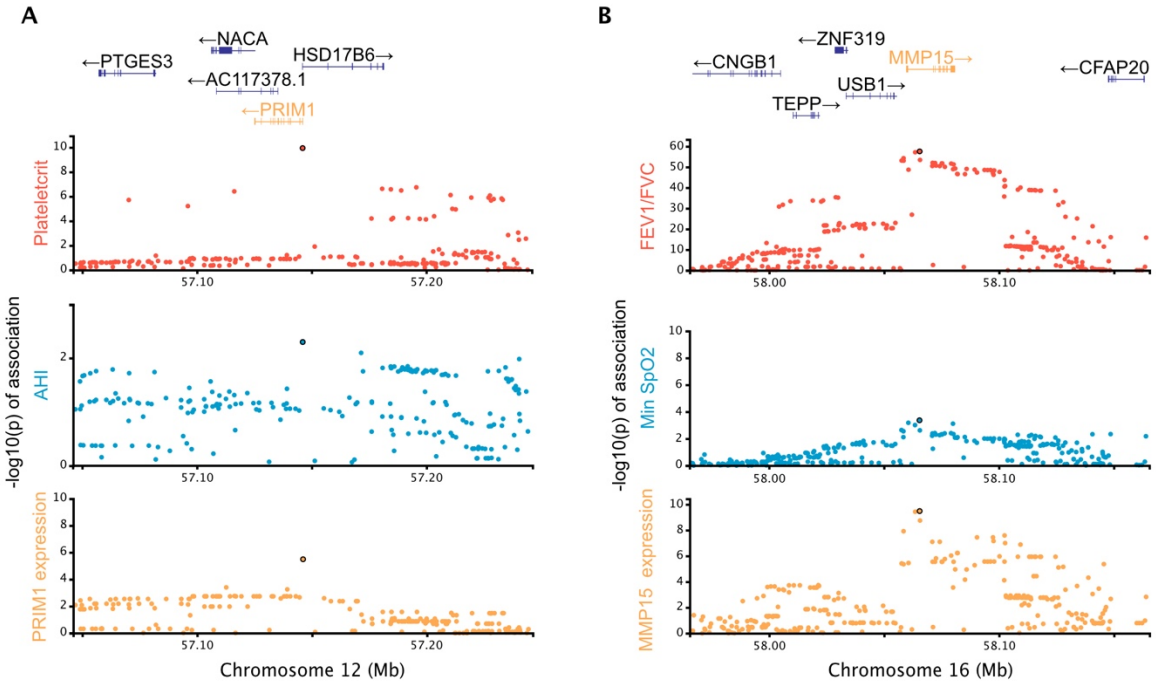

Figure 3. Candidate causal chains linking a clinical trait, OSA trait and gene expression.

A) A candidate association in chromosome 12 with putative pleiotropic associations between the plateletcrit (clinical trait; red), AHI (OSA trait; blue) and expression of *PRIM1* (DNA primase subunit 1) in monocytes (yellow). **B)** A candidate association in chromosome 16 with putative pleiotropic associations between the clinical trait FEV_1/FVC (red), minimum O_2 saturation (blue) and expression of *MMP15* (matrix metallopeptidase 15) in lung (yellow).

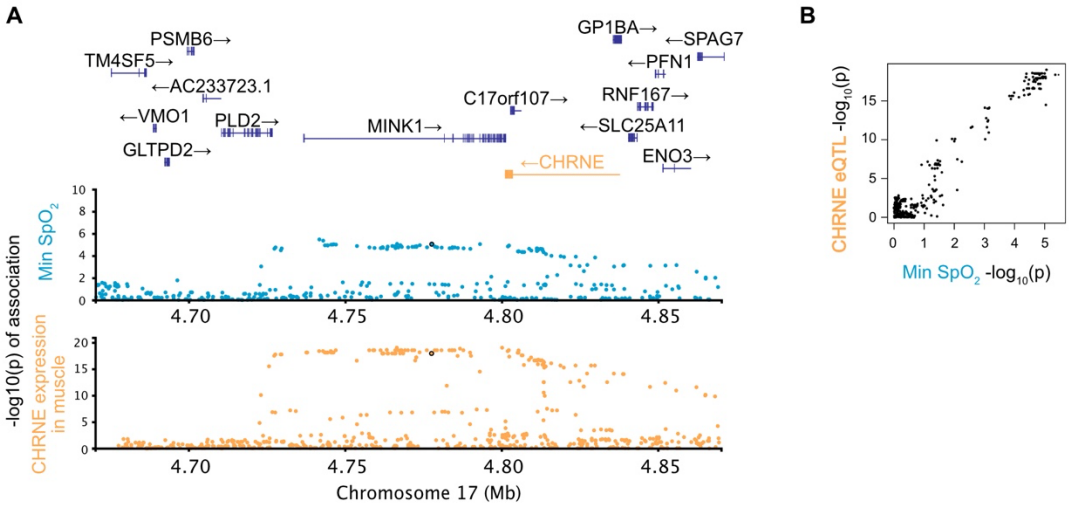

Figure 4. Pleiotropic locus linking gene expression and an OSA related trait.

A locus in chromosome 17 has associations between minimum oxygen saturation (blue) and expression of *CHRNE* (cholinergic receptor nicotinic epsilon subunit) in muscle tissues (yellow). Gene expression trait p-values and the appropriate gene in the locus are shown in yellow. Pairwise comparisons of $-\log_{10}$(p-values) between associated traits are shown in Panel **B** with matching colors in axis labels.

1377 **Table 1. Loci with significant pleiotropic associations between a clinical trait and an OSA trait with nominally significant**
1378 **replication.**
1379

SNP	Coordinate	Clinical trait	Clinical trait p-value	OSA trait	OSA trait p-value	JLIM p-value	JLIM FDR	Replication p-value
rs17010961	4:86,723,103	Systolic blood pressure	7.9E-24	Avg O2 saturation	1.6E-05	1.4E-04	0.011	7.4E-03
rs2595105	4:111,552,761	Basal metabolic rate	7.0E-13	Min O2 saturation	1.0E-03	2.4E-03	0.177	0.036
rs4711750	6:43,757,082	Granulocyte % of myeloid white cells	6.7E-09	AHI	3.2E-03	9.0E-03	0.198	0.011
		Reticulocyte fraction of red cells	6.7E-11			9.0E-03	0.108	
		High light scatter reticulocyte % of red cells	5.4E-11			1.1E-02	0.191	
rs16926246	10:71,093,392	High cholesterol	2.8E-09	Min O2 saturation	1.1E-05	3.0E-03	0.051	0.039
				Avg O2 saturation	3.5E-05	1.0E-03	0.015	1.3E-03
rs17476364 *	10:71,094,504	Hematocrit	7.7E-159	AHI	7.3E-06	3.0E-05	0.001	0.016
		Reticulocyte count	1.9E-96			3.0E-05	0.001	
		Red blood cell count	1.8E-48			3.0E-05	0.002	
		Hematocrit	7.7E-159	Avg O2 saturation	3.9E-05	4.2E-04	0.017	**8.5E-05 †**
		Reticulocyte count	1.9E-96			4.2E-04	0.019	
		Red blood cell count	1.8E-48			3.8E-04	0.020	

		Hematocrit	7.7E-159			5.0E-05	0.002	
		Reticulocyte count	1.9E-96	Min O2 saturation	3.1E-07	5.0E-05	0.002	0.014
		Red blood cell count	1.8E-48			5.0E-05	0.003	
rs11245326	10:126,357,352	White blood cell count	4.3E-09	Event Duration	9.2E-05	2.2E-03	0.057	0.017
rs2277339	12:57,146,069	Plateletcrit	1.1E-10	AHI	5.2E-03	1.0E-02	0.154	**8.2E-04 †**
		Platelet distribution width	2.4E-23			3.2E-04	0.015	
rs2297066	14:103,566,835	Mean platelet volume	7.2E-70	AHI	1.8E-03	3.9E-04	0.025	0.011
		Platelet count	4.8E-39			1.0E-03	0.064	
rs998584	6:43,757,896	Reticulocyte count	2.5E-13	AHI	1.6E-02	1.3E-02	0.133	0.016
rs765807623	14:103,571,697	Plateletcrit	7.0E-09	AHI	1.8E-03	3.8E-04	0.027	0.011

Each row denotes one SNP and its corresponding associations to clinical and OSA traits. Each SNP may be associated with more than one clinical trait. In SNPs marked with *, not all clinical traits are shown for clarity. Here, we only show variants with nominally significant replication p-values. See Table S5 for the full table of 61 loci (137 trait pairs), including those with insignificant replication p-values. Two variants marked with † indicates pleiotropic loci with significant out of sample replication p-values after Bonferroni correction (0.05/61). AHI stands for Apnea-hypopnea index. Coordinates correspond to hg19. The clinical trait p-value column refers to the association p-value of the SNP to the clinical trait. The OSA trait p-value refers to the association p-value of the SNP to the OSA trait in meta-analyzed discovery cohorts (Table S1). The replication p-value refers to the association p-value of the SNP to the OSA trait in meta-analyzed validation cohorts (Table S6). The JLIM p-value corresponds to the tests for the shared effect between the clinical and OSA phenotypes.

1391 **Table 2. Candidate causal chains.**
1392

SNP	Coordinate	Clinical trait	OSA trait	JLIM p-value	JLIM FDR	Tissue / Cell type	Gene	eQTL p-value	JLIM p-value	JLIM FDR
rs11153147	6:109,304,058	Mean corpuscular volume	Avg O2 saturation	1.1E-02	0.17	T-cell	*SESN1* (Sestrin 1)	1.4E-35	5.0E-05	0.01
						Muscle	*SESN1* (Sestrin 1)	2.6E-05	5.0E-05	0.05
						T-cell	*FOXO3* (Forkhead box O3)	1.7E-11	5.0E-05	0.01
rs4784886	16:58,065,459	FEV1/FVC	Min O2 saturation	3.4E-04	0.03	Lung	*MMP15* (Matrix metallopeptidase 15)	3.3E-10	5.0E-05	0.02
rs10160596	11:65,351,364	Mean corpuscular hemoglobin concentration	Event Duration	1.0E-02	0.17	Lung	*SCYL1* (SCY1 like pseudokinase 1)	5.1E-04	5.0E-05	0.02
rs146671954	9:136,934,203	Red cell distribution width / Sum eosinophil basophil counts	AHI	6.9E-04	0.02	Lung	*BRD3* (Bromodomain containing 3)	2.2E-07	1.0E-04	0.02
rs2277339	12:57,146,069	Plateletcrit	AHI	1.0E-02	0.15	monocyte	PRIM1 (DNA primase subunit 1)	3.2E-06	5.0E-05	0.04
						T-cell	PRIM1 (DNA primase subunit 1)	1.5E-05	5.0E-05	0.01
rs7162943	15:89,615,275	Mean platelet volume	Avg O2 saturation	1.0E-03	0.07	monocyte	*ABHD2* (Abhydrolase domain containing 2, acylglycerol lipase)	2.9E-15	1.0E-04	0.04
rs34233420	17:38,004,929	Lymphocyte count	AHI/ Min O2 saturation	3.4E-04	0.02	T-cell	*GSDMA* (Gasdermin A)	2.5E-13	5.0E-05	0.01

Each row represents a SNP with links across an OSA trait, clinical trait and gene expression trait. The link between clinical and OSA traits were thresholded at FDR < 0.2, and the link between clinical and expression traits were thresholded at FDR < 0.05. AHI stands for Apnea-Hypopnea Index. Coordinates correspond to hg19. The eQTL p-value refers to the association p-value of the SNP to the gene expression trait of the gene in the tissue/cell type indicated. The JLIM p-value corresponds to the test for the shared effect between the OSA and clinical traits (center columns) or between gene expression and the clinical trait (right columns).

1400 **Table 3. Genome-wide significant loci in OSA traits colocalizing with eQTL.**
1401

SNP	Coordinate	OSA trait	OSA assoc p-value	Gene	Tissue / cell type	eQTL p-value	JLIM p-value	JLIM FDR
rs12150370	17:4,777,634	Min O_2 Saturation	9.0E-06	*CHRNE* (cholinergic receptor nicotinic epsilon subunit)	Muscle	9.3E-20	2.0E-05	0.0006
					Neutrophil	2.5E-20	2.0E-05	0.0006
					Spleen	3.4E-13	8.0E-05	0.001
					Monocyte	8.8E-14	9.0E-05	0.001
				C17orf107 (chromosome 17 open reading frame 107)	Spleen	1.4E-08	5.0E-05	0.001

1402

1403 Three loci with known genome-wide significant association to OSA traits were tested for the shared effect with gene expression levels
1404 in seven tissue/cell types. The FDR cutoff of 0.05 was applied. The eQTL p-value refers to the association p-value of the SNP to the
1405 gene expression trait of the gene indicated, measured in the tissue/cell type indicated. The JLIM p-value refers to a pleiotropy test
1406 between the OSA and gene expression traits. See Table S7 for the full list of comparisons tested.
1407